# Simulation Research and Application on Response Characteristics of Detecting Water-filled Goaf by Transient Electromagnetic Method

**Tingye Qi**
Taiyuan University of Technology
**Xiaoming Pei**
Taiyuan University of Technology
**Guorui Feng** ( fguorui_tyut@126.com )
Taiyuan University of Technology https://orcid.org/0000-0003-4501-4214
**Huiru Wei**
Taiyuan University of Technology

**Research**

**Keywords:** transient electromagnetic method, water-accumulated goaf, forward and inverse simulation, attenuation curve of induced voltage

**Posted Date:** June 11th, 2021

**DOI:** https://doi.org/10.21203/rs.3.rs-605220/v1



**Version of Record:** A version of this preprint was published at International Journal of Coal Science & Technology on March 24th, 2022. See the published version at https://doi.org/10.1007/s40789-022-00478-0.

# Simulation Research and Application on Response Characteristics of Detecting Water-filled Goaf by Transient Electromagnetic Method

Tingye Qi[1,2], Xiaoming Pei[1,2], Guorui Feng[1,2,*], Huiru Wei[1,2]

*1. College of Mining Engineering, Taiyuan University of Technology, Taiyuan, 030024, China*

*2. Research Center of Green Mining Engineering Technology in Shanxi Province, Taiyuan, 030024, China*

**Abstract** Water inrush disasters poses a great threat to the safe exploitation of coal resources. To solve this problem, the transient electromagnetic method(TEM) was proposed to accurately detect the water accumulation in the goaf. The electromagnetic response characteristics of different water-filled goaves were studied by electromagnetic field theory, numerical simulation and field verification. Through the models of 100% water accumulation, 50% water accumulation, 0% water accumulation, 100% water accumulation with collapsed rock, 50% water accumulation with collapsed rock and 0% water accumulation with collapsed rock goaf, the characteristics of induced voltage attenuation curves were studied. Meanwhile, the relationship between the attenuation voltage value and area of the transmitting coil and the depth of the goaf were also simulated. The results illustrate that the attenuation curve of induced voltage presented a regular exponential decay form in the 0% water accumulation model but existed abnormal exaltation for voltage in water-filled model. Through the linear fitting curve, it can be seen that the abnormal intensity of the induced voltage becomes stronger as the distance between the measuring point and the center of the target decrement. Moreover, the abnormal amplitude of the induced voltage increases with the rise of the water accumulation and collapsed rock will weakly reduce the low-resistance anomalous effect on the water-accumulated goaf. In addition, the response value of the attenuation voltage increased in second-order as the area of the transmitting coil increases, but decreased in third-order as the depth of the target body increases. The field detection results of the Majiliang coal mine also confirmed the theoretical analysis and the numerical simulation. The conclusions had important guiding significance for accurate detection of coal mine goaf.

**Keywords** transient electromagnetic method, water-accumulated goaf, forward and inverse simulation, attenuation curve of induced voltage

## 1 Introduction

In China, especially in Shanxi Province, the private mining of coal resources in the past few decades has resulted in a large number of goafs with unclear locations. The accumulation of water will form water-filled goaf, which may lead to serious water disasters during normal mining activities, and bringing immeasurable life safety threats and property losses to the country and people. In view of this, it is particularly critical to propose a method to accurately locate the mined-out area of coal mine water (Wang et al. 2019; Dong 2007). At present, there are many methods for detection. Among them, the transient electromagnetic method(TEM) has the advantages of low economic cost, high efficiency, strong penetrating power of high-resistance rock formations, sensitive reflection of low-resistance bodies and unaffected by terrain conditions (Shan et al. 2009; Liu et al. 2014).Therefore, it is more appropriate to use the TEM to detect the water-accumulated goaf with low resistance response.

*Corresponding author: Feng Guorui E-mail: fguorui@163.com

As early as the 1980s, David V. Fitterman (1991) studied the electromagnetic field forward simulation calculation problem in the field of groundwater exploration, successfully detected groundwater resources on the piedmont alluvial plain in the eastern part of the city of Alain, UAE by using the ground conductivity method and the transient electromagnetic method.Kendrick Taylor (1992) used transient electromagnetic method to study the characteristics of local groundwater system in arid alluvial environment, and the false change of color apparent resistivity with time to display apparent resistivity data was adopted to determine groundwater characteristics. It can also be used in water accumulation detection. Nek R. Garg (1999) proposed a data processing of TEM based on electromagnetic field filtering to obtain a clearer geoelectric structure to determine the location of the water-filled goaf. Finally, applied it to the field detection experiment on the river plain of Idaho Snake. Jafar Sadi (2013) combined the transient electromagnetic method and the DC resistivity sounding method to identify and mapped the spatial distribution of freshwater and saline groundwater in the shallow mined-out area in the central Azraq Basin, Jordan. Reza Malekian (2019) used the finite-difference time-domain method to calculate the three-dimensional model calculation of the coal mine water goaf. The position of the goaf was distinguished by obtaining its full-space transient electromagnetic response characteristics, and the simulation results of water richness in the goaf was detected and verified in a certain mine environment. Li Chengyou and Liu Hongfu (2007) obtained the characteristics of transient electromagnetic response by analyzing the multi-channel voltage profile of transient electromagnetic and pseudo-resistivity, thereby accurately detected the location of the multi-layer (water accumulation) mined-out area. Jiang Zhihai (2014) proposed a ground-lane transient electromagnetic method (SUTEM) for laying transmitter coils on the surface and receiving by underground tunnels. 3-D unstructured tetrahedral grid vector finite element full-field electromagnetic forward algorithm was used and numerical simulations were carried out on the response of typical 1-D and 3-D water-filled goaf models. Then field tests were carried out to verify the simulation results. Tang Zhenyu (2015) proposed a transient electromagnetic imaging technology, which delineated the abnormal area of water accumulation through the two-dimensional apparent resistivity cross-section map and the slice map. The detection example of the water-accumulated goaf in the $10^{\#}$ coal seam of Shanxi showed the imaging technology can accurately locate the range and state of the abnormal area of stagnant water. Chang Jianghao (2017) established a full-space geoelectric model of the mined-out area based on the coal-measure stratigraphic data in North China and the Middle East. The convolutional perfectly matched layer (CPML) was chosen as the boundary condition and simulated the overall transient electromagnetic response of the coal mine water-bearing subsidence column at different depths of the stope floor and in front of the driving work with the finite difference time domain method. Yu Chuantao (2018) improved the traditional large fixed source loop device in the ground TEM, and applied it to the detection of the water-filled goaf of a coal mine in Shanxi. The apparent resistivity section was obtained through inversion to obtain the electromagnetic response, and the drilling verification had accurately positioned the buried depth of 300m in the mined-out area with water. Yan Guocai (2020) used electrical source short-offset transient electromagnetic method to detect deep low-resistance water accumulation areas with buried depth of more than 1000m. Response characteristics of regional apparent resistivity and the law of sounding through inversion calculation of the H-type theoretical model were obtained by an improved least square method. Moreover, this method was applied to detect the goaf of the thick conglomerate layered water in the deep part of the North China mining area.

In summary, many achievements about TEM detection of water-filled goafs has been aquired. However, there are relatively few studies on the electromagnetic response characteristics for goaf with complicated accumulated water occurrence states. In this paper, theoretical analysis and numerical simulation are used to obtain the transient electromagnetic response characteristics of the goaf under different water accumulation conditions, and field tests are performed to verify the simulation results. At the same time, the research results provide theoretical and technical support for the accurate detection of water-filled goafs and coal mine safety production.

## 2 Theory of transient electromagnetic field for water-filled goaf detection

### 2.1 Theory of electromagnetic field

Almost all theories of electromagnetic phenomena are derived on the basis of Maxwell's equations. TEM belongs to the time-domain electromagnetic detection method and also complies with the basic equations.

$$\begin{aligned} \nabla \times E &= -\frac{\partial B}{\partial t} \\ \nabla \times H &= j + \frac{\partial D}{\partial t} \\ \nabla \cdot B &= 0 \\ \nabla \cdot D &= \rho \end{aligned} \tag{1}$$

Three matter equations as follow

$$j = \sigma E \quad B = \mu H \quad D = \varepsilon E \tag{2}$$

Where $E$ is electric field intensity(V/m), $B$ is the magnetic induction intensity(Wb/m$^2$), $H$ is the magnetic field intensity (A/m), $D$ is the electric displacement vector($C$/m$^2$), $j$ is the current density (A/m$^2$), $\rho$ is the free charge density, $\sigma$ is the electrical conductivity, $\mu$ is the magnetic permeability, $\varepsilon$ is the dielectric constant. Maxwell's equation characterizes the relationship between field strength vector, current density and charge density.

**2.2 Calculation of transient electromagnetic field response**

According to the relevant research of experts (Li 2002; Luo 2012; Bai 2003), based on the calculation theory of the electromagnetic field in the frequency domain, the Fourier inverse solution is the best calculation method, so this research also follows this. In order to simplify the calculation process, the cylindrical symmetry of the electromagnetic field is usually chosen to solve the electromagnetic parameters, and the Hertzian potential function F is also introduced as

$$F_1(r,z) = \frac{I_0 a}{2}\int_0^\infty \frac{2\lambda}{\lambda + u_1} e^{-u_1 h} J_1(\lambda a) J_0(\lambda r) d\lambda \tag{3}$$

The expression of the frequency domain electromagnetic field component are follows

$$\begin{aligned} E_\phi(\omega) &= -i\omega\mu \frac{\partial F}{\partial r} = i\omega\mu I_0 a \int_0^\infty e^{-u_1 h} \frac{\lambda}{\lambda + u_1} J_1(\lambda a) J_1(\lambda r) d\lambda \\ H_r(\omega) &= \frac{\partial^2 F}{\partial r \partial z} = -I_0 a \int_0^\infty e^{-u_1 h} \frac{\lambda^2}{\lambda + u_1} J_1(\lambda a) J_1(\lambda r) d\lambda \\ H_z(\omega) &= -\frac{1}{r}\frac{\partial}{\partial r}\left(r\frac{\partial F}{\partial r}\right) = I_0 a \int_0^\infty e^{-u_1 h} \frac{\lambda^2}{\lambda + u_1} J_1(\lambda a) J_0(\lambda r) d\lambda \end{aligned} \tag{4}$$

Replace the induced electromagnetic field at any point by induced electromagnetic field of the center loop, at this time r = 0, $J_0(0) = 1$, $J_1(0) = 0$, formula (4) can be written as

$$H_Z(\omega) = \frac{I_0}{k_1^2 a^3}\left[3 - \left(3 + 3k_1 a + k_1^2 a^2\right) e^{-k_1 a}\right] \tag{5}$$

In the equation, $a$ is the radius of the coil, $I_0$ is the emission current, $k_1$ is the wave number, $k_1^2 = -i\omega\sigma\mu_1$ , $u_1$ is the auxiliary parameter, $u_1 = \sqrt{\lambda^2 + k_1^2}$ , $\mu_1$ is the permeability of the underground goaf, $J_0(\lambda a)$ is the first kind of zero-order Bessel function, $J_1(\lambda r)$ is the first-order Bessel function of the first kind, $\sigma$ is the uniform conductivity of underground space.

When the mined-out area contains water, the dielectric constant $\varepsilon$, magnetic permeability $\mu$ and resistivity $\rho$ will change as follows

$$\varepsilon = \varepsilon_0 \cdot \varepsilon_r \quad \mu = \mu_0 \cdot \mu_r \quad \rho = \rho_w \cdot \frac{3 - w_1}{2w_1} \tag{6}$$

Where $\varepsilon_0 = (1/36\pi) \times 10^{-9}$ F/m is the vacuum dielectric constant, $\varepsilon_r$ is the relative dielectric constant which depends on the specific rock conditions after water accumulation in the goaf. $\mu_0 = 4\pi \times 10^{-7}$ is the vacuum permeability, $\mu_r$ is the relative permeability, $\rho_w$ is the resistivity of water-filled goaf, $w_1$ is the water content of the rock.

Establishing the conversion relationship between frequency response and time domain response

$$\begin{aligned} H(t) &= \frac{1}{2\pi}\int_{-\infty}^{\infty} \frac{H(\omega)}{-i\omega} e^{-i\omega} d\omega \\ \frac{\partial B_z(t)}{\partial t} &= \frac{1}{2\pi}\int_{-\infty}^{\infty} \frac{\frac{\partial B_z(\omega)}{\partial t}}{-i\omega} e^{-i\omega} d\omega \end{aligned} \tag{7}$$

In practical applications, transient electromagnetic instruments generally receive induced electromotive force signals $\varepsilon(t) = \frac{\partial H_z(t)}{\partial t}$. According to the previous calculation method, the following expression is described as

$$\frac{\partial H_z(\omega)}{\partial t} = -i\omega H_z(\omega) = \frac{3I_0\rho}{\mu_1 a^3}\left[1 - \left(1 + k_1 a + \frac{1}{3}k_1^2 a^2\right) e^{-k_1 a}\right] \tag{8}$$

After inverse Fourier transform, the equations are

$$\frac{\partial H_z(t)}{\partial t} = \frac{3I_0\rho_w(3 - w_1)}{2w_1\mu_1 a^3}\left[\Phi(u) - \sqrt{\frac{2}{\pi}}u\left(1 + \frac{u^2}{3}\right)e^{-\frac{u^2}{2}}\right] \tag{9}$$

$$\frac{\partial B_z(t)}{\partial t}=\mu\frac{\partial H_z(t)}{\partial t}=\frac{3I_0\rho_w(3-\omega)}{2\omega a^3}\left[\Phi(u)-\sqrt{\frac{2}{\pi}}u\left(1+\frac{u^2}{3}\right)e^{-\frac{u^2}{2}}\right] \quad (10)$$

$$\Phi(u)=\sqrt{\frac{2}{\pi}}\int_0^{u(t)}e^{-\frac{t^2}{2}}dt \quad (11)$$

Where a is the radius of the circular coil (if the transmitting coil is a square coil with side length L, then $a=L/\sqrt{\pi}$), $u$ is the comprehensive parameter, $u=2\pi a/\tau$, $\tau$ is the apparent diffusion parameter, $\tau=2\pi\sqrt{2\rho t/\mu_0}$, $\mu_1$ is the permeability of the mined-out layer of water, $\mu_0$ is magnetic permeability in vacuum, $t$ is the diffusion time of the transient field, $\rho_w$ is the resistivity of the groundwater goaf, $\Phi(u)$ is the probability integral.

### 2.3 Theoretical calculation

According to equation (10) and (11), MATLAB is used for programming (Tong 2013) to study the transient electromagnetic response characteristics of the goaf under different water accumulation conditions. The basic parameters are set that the coil radius a is 100m, the emission current is 1A, the surrounding rock resistivity of the goaf area is 500Ω·m, $\mu_0$ = 4π×10-7 H/m. The resistance of the mined-out layer are selected as $\rho_1$=5Ω·m(fully-water-filled),$\rho_2$=50Ω·m(half-water-filled), and $\rho_3$ = 1000Ω·m (water-unfilled) respectively. $t$ is the diffusion time, ranging from 0.1ms to 100ms.The coordinate axis is expressed in double logarithmic form, and the attenuation voltage curves under the three models are shown in Figure 1.

The attenuation trend of the three curves is similar and the attenuation voltage response value is proportional to the amount of water accumulation. It also shows that the greater the amount of water accumulation, the higher the voltage value.

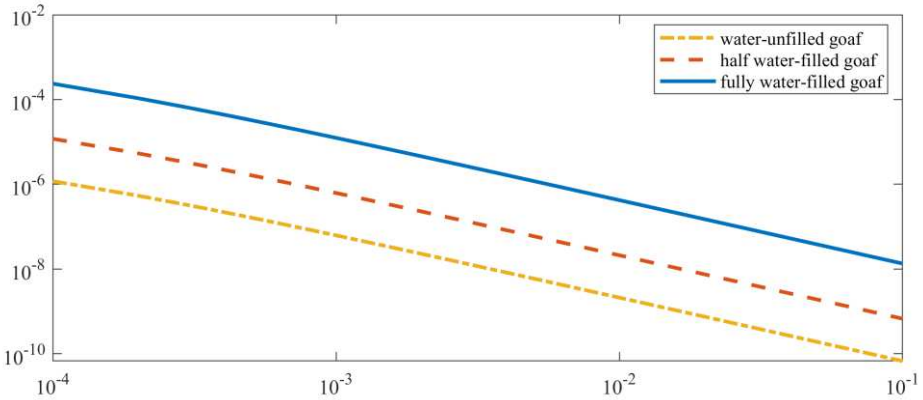


**Fig.1** Attenuated voltage curve of the water-filled goaf under different states

## 3 Numerical simulation of transient electromagnetic response of water-filled goaf in different states

### 3.1 Goaf model of water-filled states

Coal mine goaf is the closed or semi-enclosed space area left behind by the underground coal seam being mined. After the goaf formed, the integrity of the rock strata is destroyed, causing a large area of cracks inside the rock strata. When the goaf is filled with water, its resistivity is lower than the surrounding rock. When the goaf does not contain water, the regional resistivity is higher than that of the surrounding rock. Simulation research is carried out based on the physical characteristics (Han 2018, Lian 2020).

The simulation was used Maxwell software for calculation. In order to truly reflect the changes in the water environment in the mined-out area, the plate-shaped structure was selected to simulate the various underground rock layers and 6 goaf models of 100% water accumulation, 50% water accumulation, 0% water accumulation, 100% water accumulation with collapsed rock, 50% water accumulation with

collapsed rock and 0% water accumulation with collapsed rock were established. Then the electromagnetic response characteristics were analyzed through the attenuation electromotive force curve and apparent resistivity cross-section obtained by forward and inversion simulation.

### 3.2 Transient electromagnetic response characteristics of goaf models in different water-accumulated states

In this study, the water-accumulated goaf of Majiliang mining area in Datong is selected as the research object, the forward model is established by referring to the site geological conditions and the electrical properties of the overlying rock and floor layer of the goaf

The detection coil is selected center loop coil and basic parameters of the model have been set after several tests. The emission current is 1A, the transmission frequency is 8Hz, the turn number is 1, the side length of the transmitting coil is 100m, and the receiving device selects a probe with an equivalent area of 10000m$^2$. Moreover, the sampling time is 53ms, the number of channels is 30, and the amounts of measuring lines and points are 1 and 21 respectively. The distance between the measuring points is 25m. The total latera measured distance ranges from 0 to 500m. Each plate-shaped body is centered at a lateral position of 250m.The survey line is 200m horizontally and 100m in the direction (vertical to the survey line).

Figure 2(a) shows the schematic diagram of the model of the 100% water accumulation goaf. According to the buried depth from shallow to deep, it is divided into three layers of geological bodies called overlying rock layer, water-filled goaf layer, and floor layer, corresponding to the resistivity of each layer is 1000Ω·m, 5Ω·m and 200Ω·m, and the thickness is 100m, 20m and 50m respectively. The rest of the space is considered as the surrounding rock, the resistivity is 500Ω·m while the thickness is infinite, and the subsequent models are also the same.

Figure 2(b) shows the schematic diagram of the model of the 50% water accumulation goaf. According to the buried depth from shallow to deep, it is divided into four layers of geological bodies called overlying rock layer, goaf layer, water-filled goaf layer, and floor layer, corresponding to the resistivity of each layer is 1000Ω·m, 2000Ω·m, 5Ω·m and 200Ω·m, and the thickness is 100m, 10m, 10m and 50m respectively.

Figure 2(c) shows the schematic diagram of the model of the 0% water accumulation goaf. According to the buried depth from shallow to deep, it is divided into three layers of geological bodies called overlying rock layer, goaf layer, and floor layer, corresponding to the resistivity of each layer is 1000Ω·m, 2000Ω·m and 200Ω·m, and the thickness is 100m, 20m and 50m respectively.

Figure 2(d) shows the model diagram of the 100% water accumulation with collapsed rock. It is divided into three geological bodies of overlying rock layer, water-filled goaf layer and floor layer according to the buried depth from shallow to deep, corresponding to the resistivity of each layer is 1000Ω·m, 2000Ω·m and 200Ω·m, and the thickness is 100m, 20m and 50m respectively. The collapsed rock exists in the mined-out area which is set the length of 100m and thickness of 10m, and the resistivity of the collapsed rock mass is 1000Ω·m.

Figure 2(e) shows the model diagram of the 50% water accumulation with collapsed rock. It is divided into four geological bodies of overlying rock layer, goaf layer, water-filled goaf layer and floor layer according to the buried depth from shallow to deep, corresponding to the resistivity of each layer is 1000Ω·m, 2000Ω·m, 5Ω·m and 200Ω·m, and the thickness is 100m, 10m, 10m and 50m respectively.

Figure 2(f) shows the model diagram of the 0% water accumulation with collapsed rock. It is divided into three geological bodies of overlying rock layer, goaf layer and floor layer according to the buried depth from shallow to deep, corresponding to the resistivity of each layer is 1000Ω·m, 2000Ω·m and 200Ω·m, and the thickness is 100m, 20m and 50m respectively.

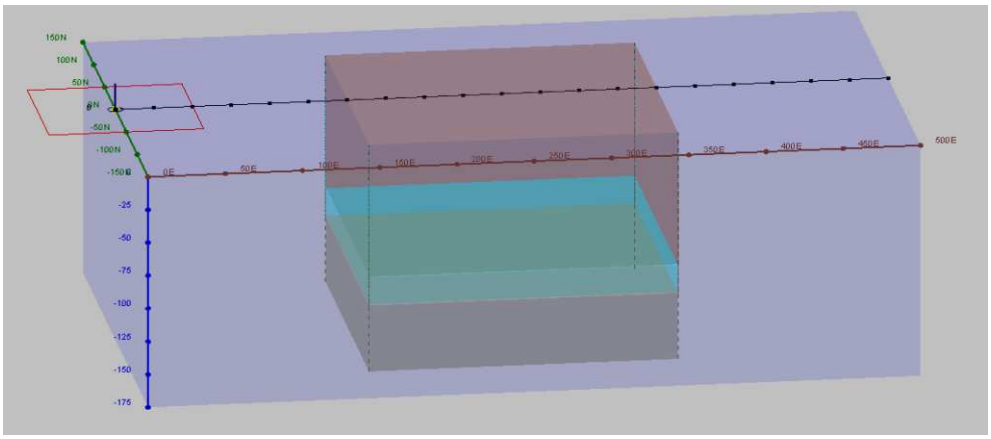
150N
100N
50N
0N
-50N
-100N
-150N
0E
50E
100E
150E
200E
250E
300E
350E
400E
450E
500E
-25
-50
-75
-100
-125
-150
-175

(a)

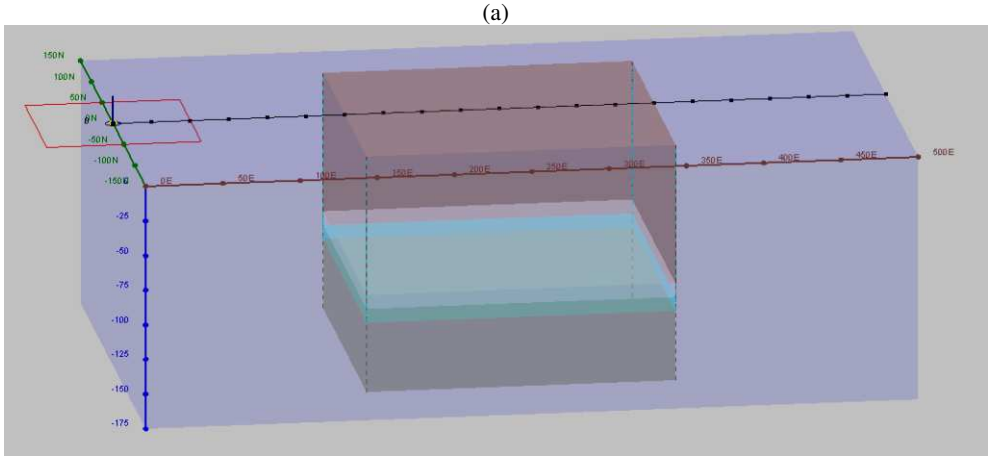
150N
100N
50N
0N
-50N
-100N
-150N
0E
50E
100E
150E
200E
250E
300E
350E
400E
450E
500E
-25
-50
-75
-100
-125
-150
-175

(b)

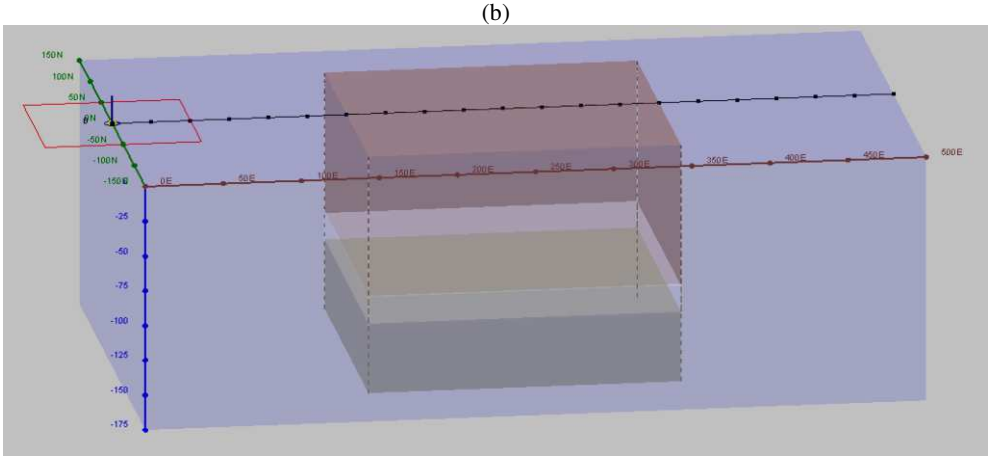
150N
100N
50N
0N
-50N
-100N
-150N
0E
50E
100E
150E
200E
250E
300E
350E
400E
450E
500E
-25
-50
-75
-100
-125
-150
-175

(c)

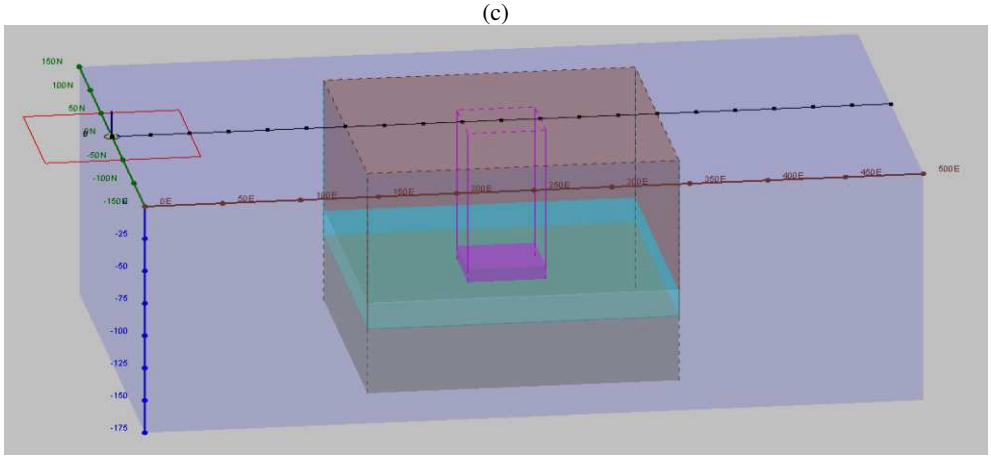
150N
100N
50N
0N
-50N
-100N
-150N
0E
50E
100E
150E
200E
250E
300E
350E
400E
450E
500E
-25
-50
-75
-100
-125
-150
-175

(d)

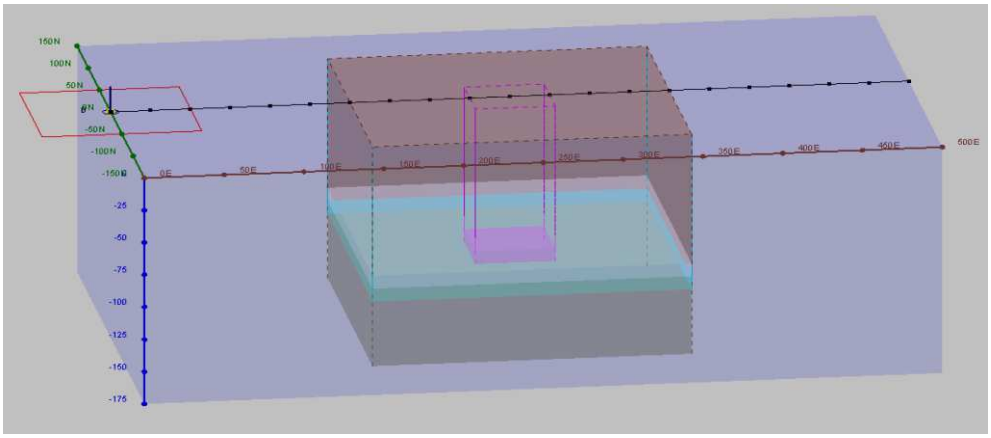


(e)

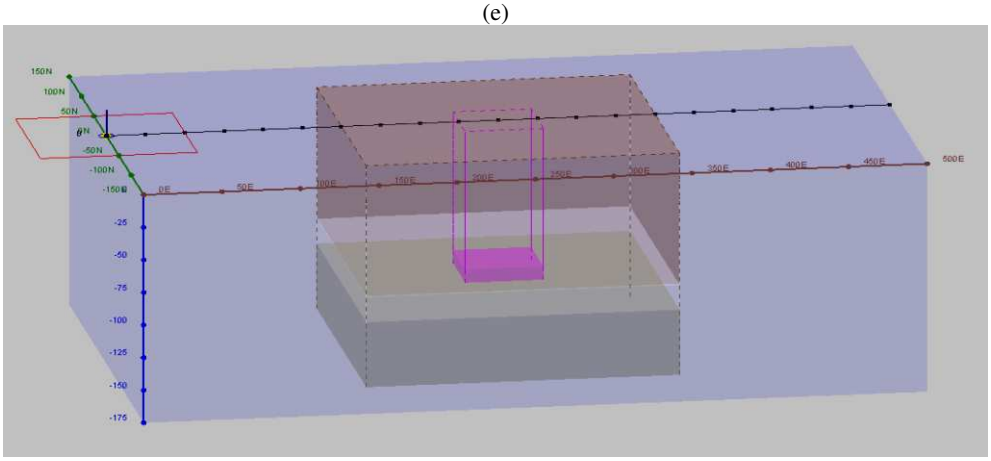


(f)

**Fig.2** Model of the water-filled goaf under different states: (a) Model of the 100% water accumulation goaf, (b) Model of the 50% water accumulation goaf, (c) Model of the 0% water accumulation goaf, (d) Model of the 100% water accumulation with collapsed rock goaf, (e) Model of the 50% water accumulation with collapsed rock goaf, (f) Model of the 0% water accumulation with collapsed rock goaf

According to the forward simulation calculation, the attenuation voltage curve of each model is obtained to reflect the transient electromagnetic response characteristics. The curve was expressed in double logarithmic coordinates, the ordinate is the normalized attenuation voltage response value, and the abscissa is the sampling time. In order to clearly reflect the response characteristics, we select the six points at the horizontal distance of 50m, 100m, 125m, 150m, 175m and 250m on the survey line to observe.

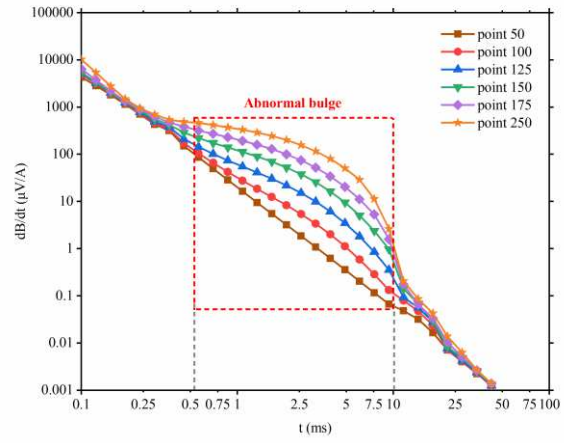


(a)

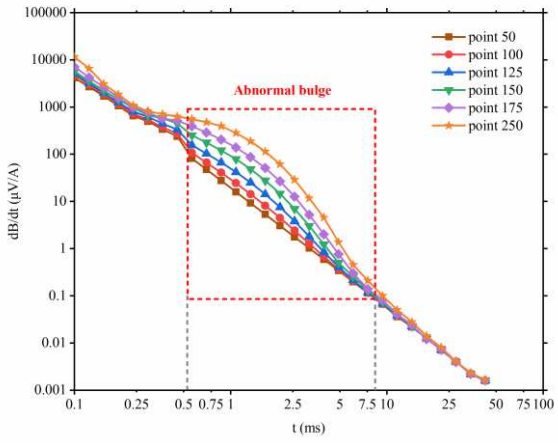


(b)

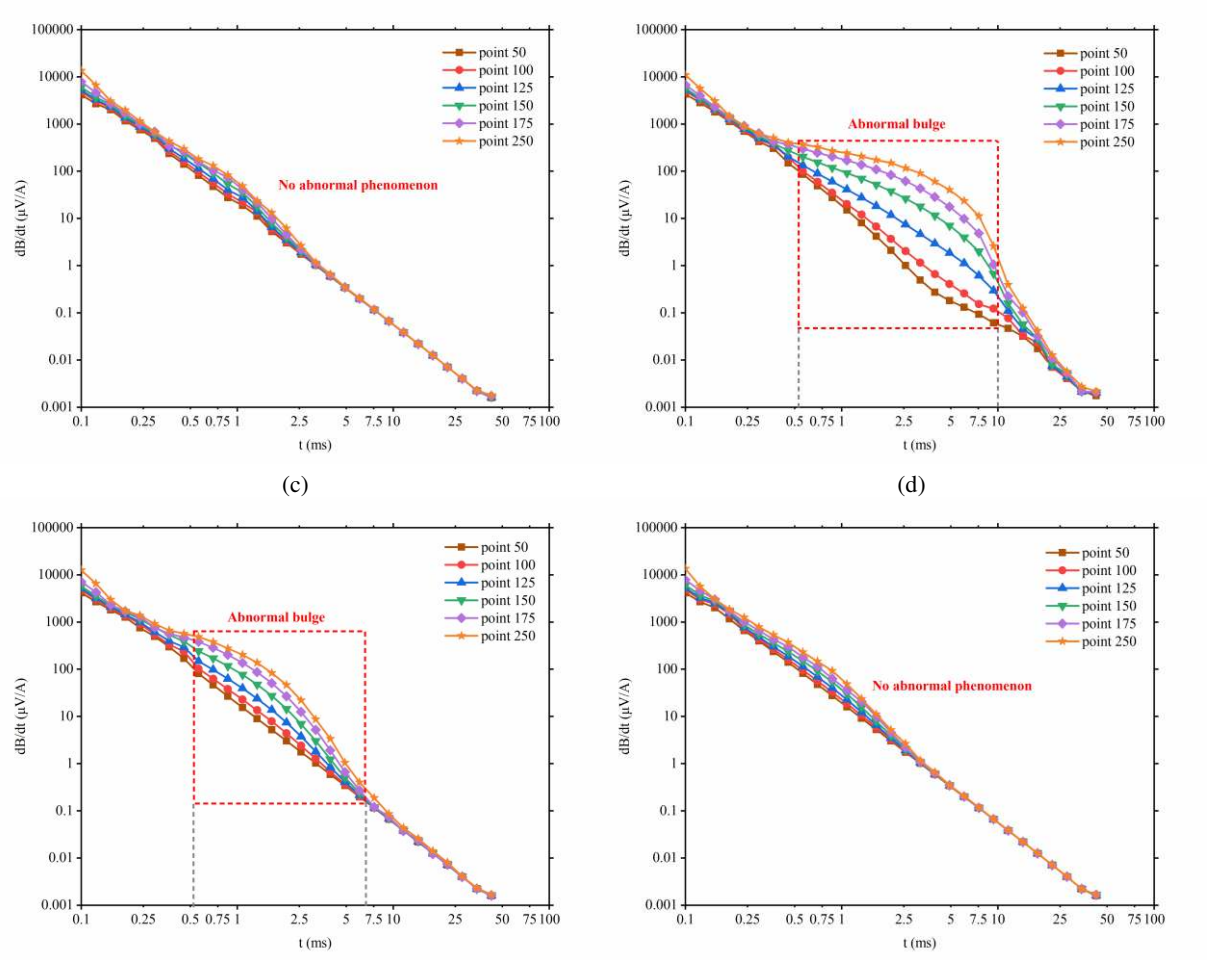


**Fig.3** Attenuated voltage curve of water-filled goaves in different states: (a) Model of the 100% water accumulation goaf, (b) Model of the 50% water accumulation goaf, (c) Model of the 0% water accumulation goaf, (d) Model of the 100% water accumulation with collapsed rock goaf, (e) Model of the 50% water accumulation with collapsed rock goaf, (f) Model of the 0% water accumulation with collapsed rock goaf

The attenuation voltage curves of the six conditions of water accumulation were selected. The voltage curve will show obvious "bulge" abnormal reflection when goaf contains water, and the shape presents "S" type. The closer the measurement point is to the upper part of the water in the goaf, the more obvious the abnormal response, which indicates that TEM has a stronger ability to distinguish low-resistance anomalies containing water, as shown in Figure 3 (a) and 3 (b). The voltage curves almost overlap when the goaf is water-unfilled, the attenuation trend is similar, and the curve presents the characteristics of an exponential attenuation curve that indicates TEM has no obvious abnormal response to the unfilled high-resistance target, as shown in Figure 3(c). The collapsed rock is formed by the landsliding of the roof, and its resistivity is extremely high compare to the surrounding rock. If water and collapsed bodies both contain in the mined-out area, the attenuation curve still produces a relatively large "bulge" anomaly. However, the abnormal response is weakened, and the voltage value is correspondingly reduced. It can be known that when the water and the collapsed body exist at the same time, the impact of the water on the attenuation voltage response is more significant, and the collapsed body can only reduce the abnormal amplitude, as shown in Figure 3(d) and 3(e). When the goaf has collapsed rock with 0% water accumulation, the target body shows extremely high resistance, and the attenuation voltage curve is not abnormal. The attenuation trend of curve is consistent with the water-unfilled goaf model, as shown in Figure 3(f).

Linear fitting is performed for the attenuation voltage curve of the above water accumulation model,

taking the 100% water accumulation mined-out area as an example, the fitted curve is shown in Figure 4. The number of the measuring point indicates the horizontal distance from the origin of the measuring point. It can be seen from the figure that all the fitted curves are in a linear function distribution, and the slope of the curve increases with the increment of the number of measuring points, while the fit degree of the curve becomes worse, and the $R^2$ value continues to decrease. When the measuring point distance is 250m, the $R^2$ value is only 0.848. It indicates that the attenuation curve located in the center of the water-filled goaf has the strongest anomalous response.

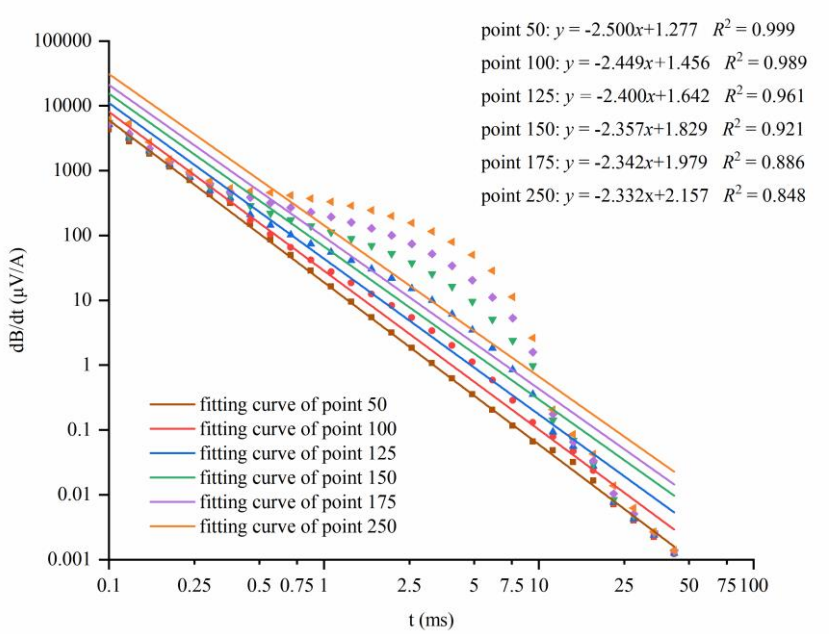


**Fig.4** The fitting curve of the attenuation voltage of measuring points in 100% water accumulation goaf

According to the attenuated voltage response of the forward modeling, the apparent resistivity profile diagrams of six types of water-filled goafs were obtained by inversion calculation. There is an inverse proportional relationship between the apparent resistivity value and the induced electromotive force response value. The abscissa shows the lateral distance position of the measuring point, and the ordinate shows the depth of burial. The colorimetric scale chart below shows the apparent resistivity value and color deepens and increases continuously.

When the goaf is completely filled with water, an abnormally low-resistance enclosed area appears at the buried depth of -100m to -130m and the measuring point distance of 150m to 350m (water-filled goaf). The abnormal increment for the induced electromotive force lead to the decrement of apparent resistivity value when the goaf is fully water-filling. Corresponding to the above-mentioned forward modeling results, the apparent resistivity contour lines around are distributed in irregular shapes, as shown in the Figure 5(a). When the goaf contains 50% water, the high-resistance air layer will weaken the abnormal amplitude. Compared with the full-water model, a small anomaly low-resistance enclosed area will generate at the buried depth -105m to -120m and the lateral distance from 175m to 330m, as shown in Figure 5(b). When there is no water in the mined-out area, no obvious enclosed area appear on the apparent resistivity profile diagram, the resistance of each layer is linearly distributed, and the value is high. This is because the induced electromotive force does not increase abnormally, while the apparent resistivity value did not decrease significantly, as shown in Figure 5(c).

For the mined-out area with collapsed rock mass, based on the slight difference of the induced voltage response, and the trend of the apparent resistivity profile obtained from the inversion is almost the same as that mind-out area without collapsed rock. The resistivity value has little increment, as shown in Figure 5(d)-5(f).

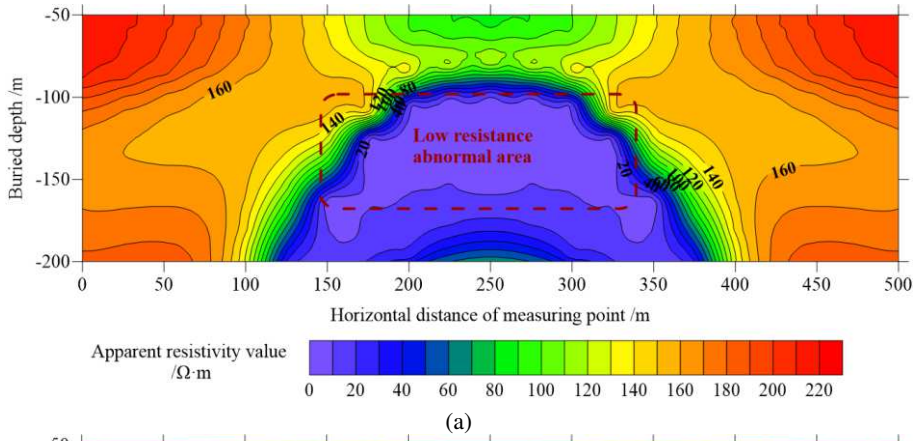
Buried depth /m
-50
-100
-150
-200
0 50 100 150 200 250 300 350 400 450 500
Horizontal distance of measuring point /m
Low resistance abnormal area
160
140
120
100
80
60
40
20
Apparent resistivity value /Ω·m
0 20 40 60 80 100 120 140 160 180 200 220

(a)

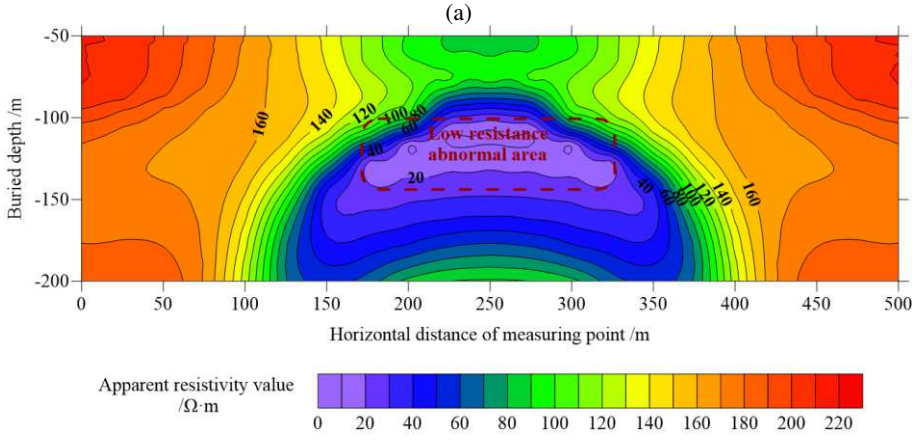
Buried depth /m
-50
-100
-150
-200
0 50 100 150 200 250 300 350 400 450 500
Horizontal distance of measuring point /m
Low resistance abnormal area
160
140
120
100
80
60
40
20
Apparent resistivity value /Ω·m
0 20 40 60 80 100 120 140 160 180 200 220

(b)

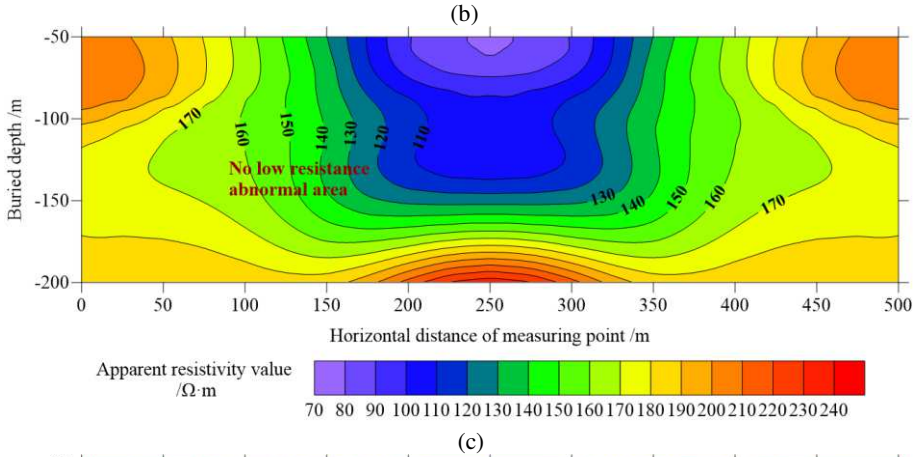
Buried depth /m
-50
-100
-150
-200
0 50 100 150 200 250 300 350 400 450 500
Horizontal distance of measuring point /m
No low resistance abnormal area
170
160
150
140
130
120
110
Apparent resistivity value /Ω·m
70 80 90 100 110 120 130 140 150 160 170 180 190 200 210 220 230 240

(c)

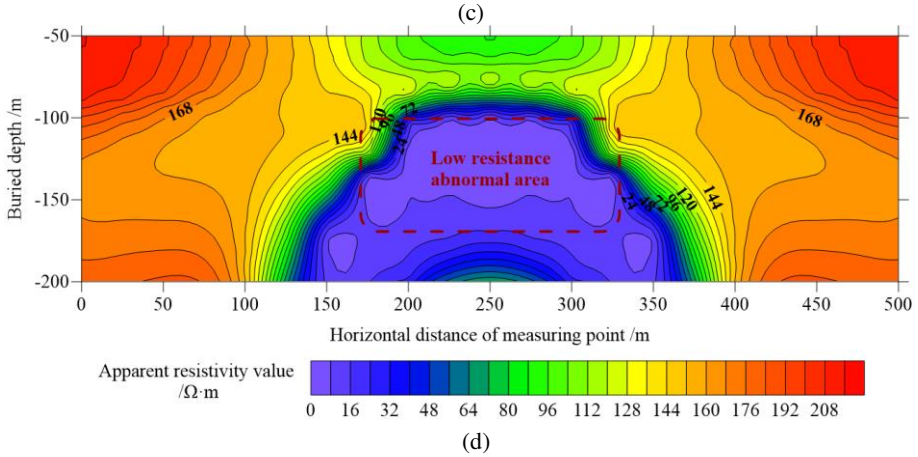
Buried depth /m
-50
-100
-150
-200
0 50 100 150 200 250 300 350 400 450 500
Horizontal distance of measuring point /m
Low resistance abnormal area
168
144
120
Apparent resistivity value /Ω·m
0 16 32 48 64 80 96 112 128 144 160 176 192 208

(d)

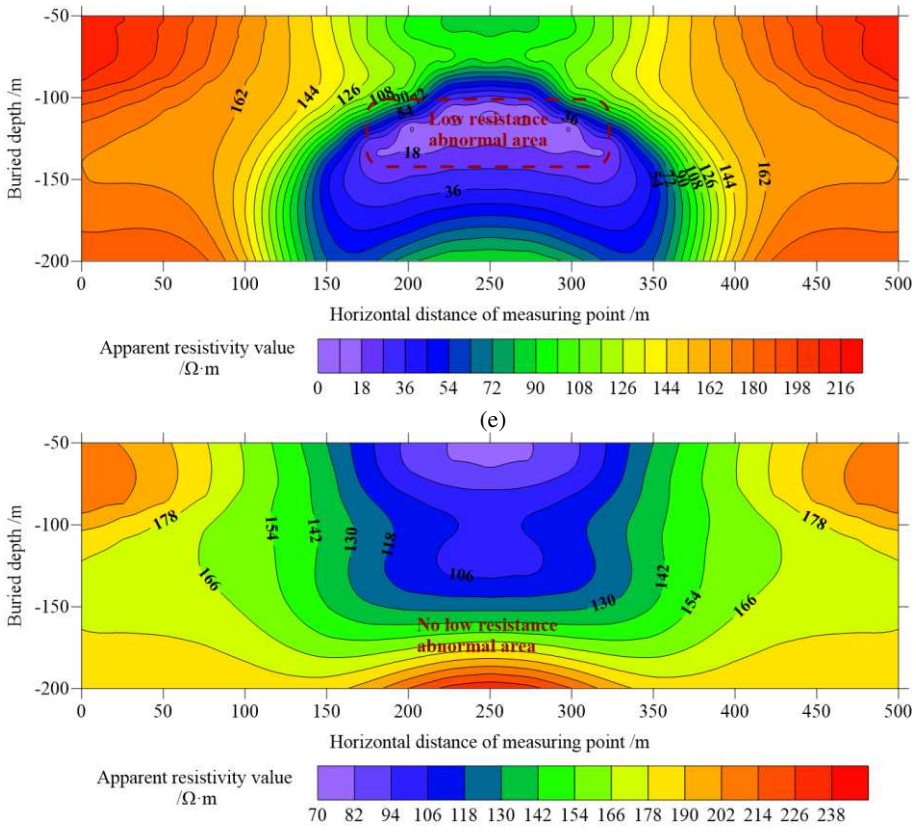


**Fig.5** The apparent resistivity cross-section diagrams of the goaf with water accumulation in different states: (a) Model of the 100% water accumulation goaf, (b) Model of the 50% water accumulation goaf, (c) Model of the 0% water accumulation goaf, (d) Model of the 100% water accumulation with collapsed rock goaf, (e) Model of the 50% water accumulation with collapsed rock goaf, (f) Model of the 0% water accumulation with collapsed rock goaf

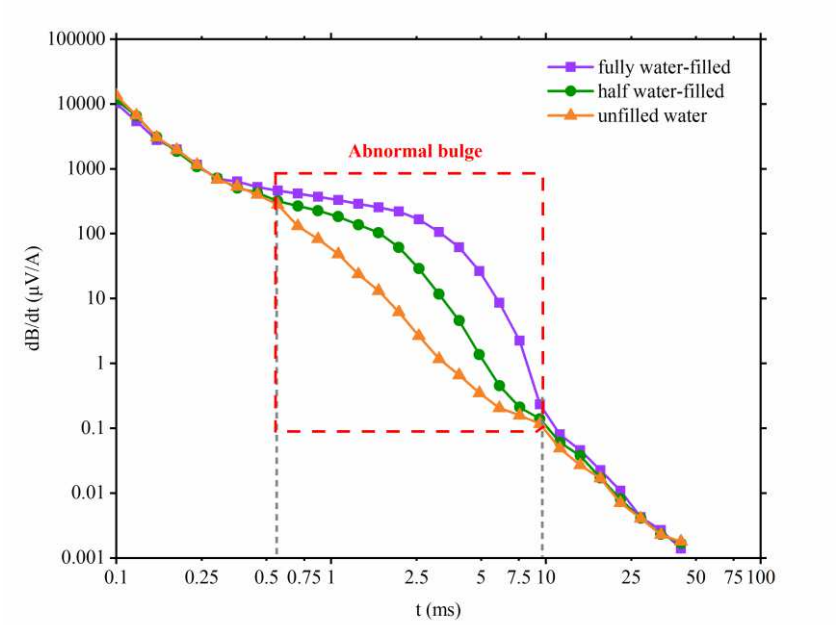


**Fig.6** Attenuation voltage curves under different amounts of accumulated water

To analyze the influence of three states for 100% water accumulation goaf, 50% water accumulation goaf and water-unfilled goaf on the voltage response value, we selected the attenuation curve generated at the measurement point (250 m) with the strongest response characteristic for analysis.

The attenuation voltage curve under different water accumulation conditions is shown in Figure 6. The

response value of the attenuation voltage depends on the resistance value of the formation at different buried depths. Since the overburden setting of each model is the same, the initial response values (at 0.1ms-0.5ms)of the three goaf models under the conditions of water accumulation are basically analogous. Afterwards, due to the low resistance characteristics of the water accumulation, the induced voltage curve will produce abnormal "bump" phenomenon within the sampling time of 0.56ms~10ms. The attenuation process is limited and the sequence of the degree of abnormal response is 100% water accumulation goaf > 50% water accumulation goaf > 0% water accumulation goaf. Which implys that the larger the amount of water accumulation, and brought the more obvious the low resistance effect. Moreover, the attenuation rate of the induced electromotive force response is slower while the response value is higher.

### 3.3 Transient electromagnetic response characteristics of water-filled goaf with different coil sizes

This section studies the electromagnetic response characteristics of six goaf models under different transmitter coil sizes. The working parameters are set as follows: the emission current is 1A, the emission frequency is 8Hz, the number of turns is 1, the sampling time is 53ms, and the number of time channels is 30. The side lengths of the single-turn transmitting coils is set to 100m, 150m, 200m and 400m respectively, and the receiving coils were selected with an equivalent area of 10000m$^2$ to perform forward calculations on each goaf model, as shown in Figure 7(a)~(f).

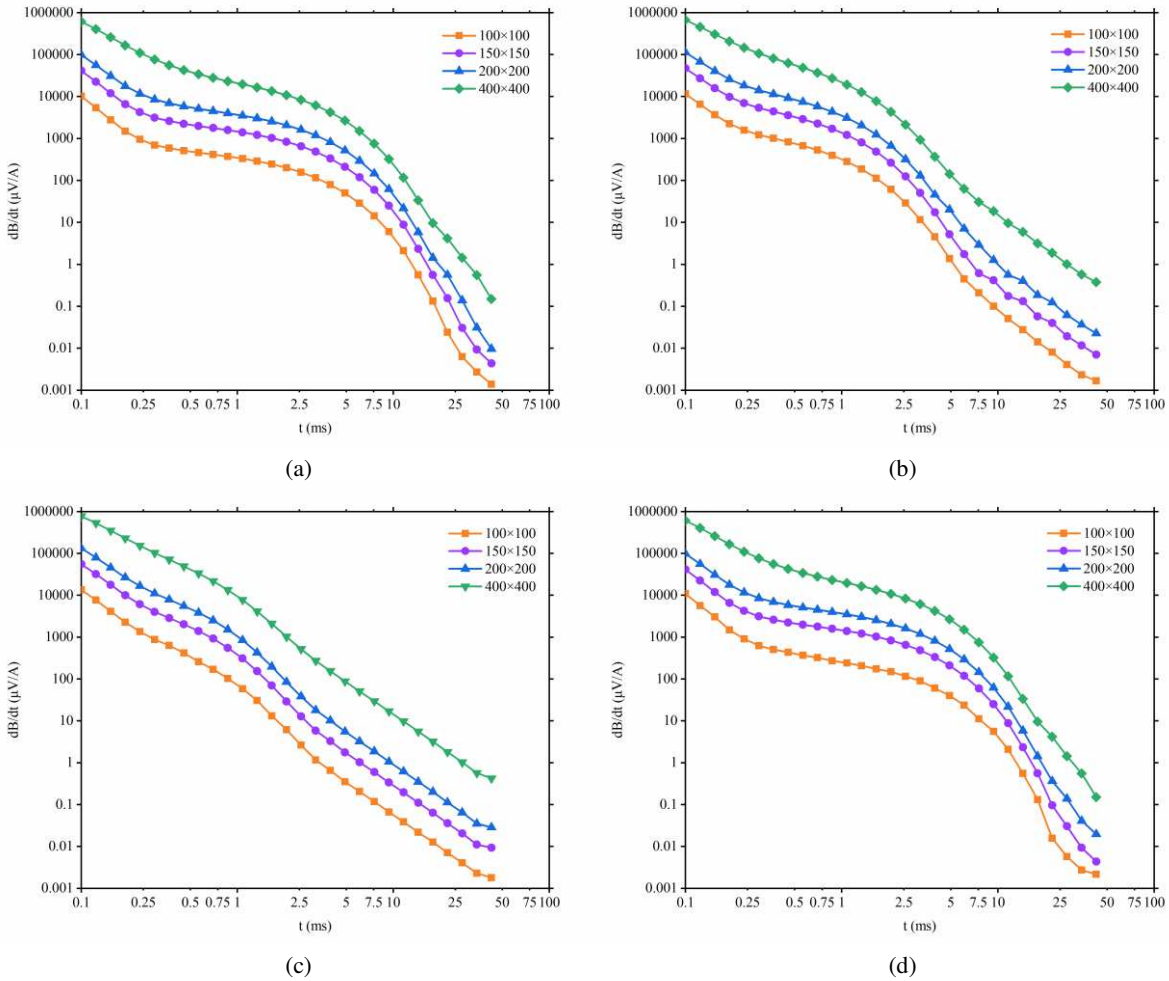

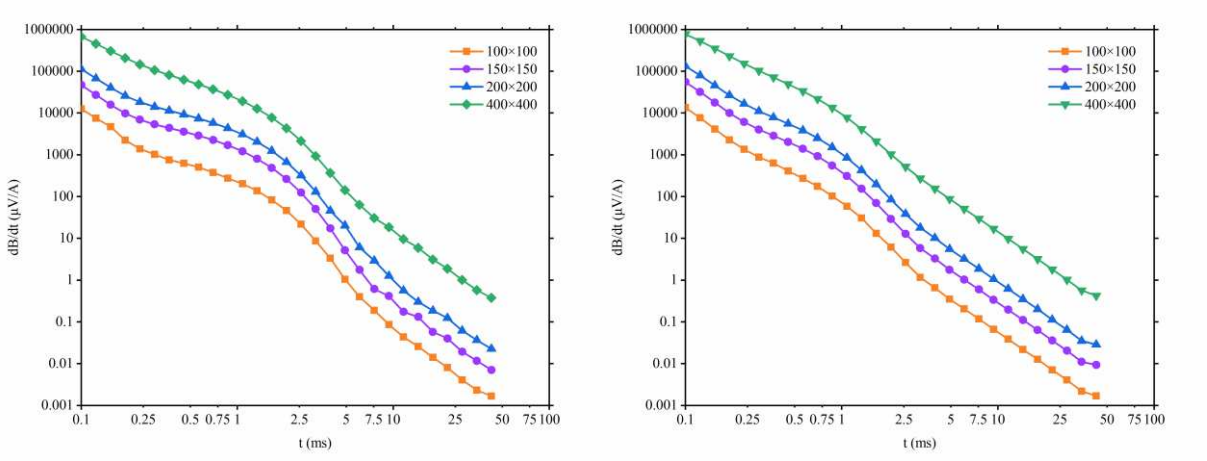


(e) (f)

**Fig.7** Attenuated voltage curves of the different water-filled goaf models with different coil sizes: (a) Model of the 100% water accumulation goaf, (b) Model of the 50% water accumulation goaf, (c) Model of the 0% water accumulation goaf, (d) Model of the 100% water accumulation with collapsed rock goaf, (e) Model of the 50% water accumulation with collapsed rock goaf, (f) Model of the 0% water accumulation with collapsed rock goaf

It can be seen from the figure that the initial voltage values of the six models of water-filled goafs increase significantly with the continuous increase of the side length of the transmitting coil. When the coil side length is 100m, the initial value of the attenuation voltage is about 11000~13000μV/A. When the coil side length is 150m, it is about 41000~55000μV/A. When the coil side length is 200m, the voltage value is about 98000~130000μV/A while it rises to 610000~770000μV/A when the side length of the coil is 400m. However, the attenuation trends of the four voltage curves are almost consistent, and the abnormal "upward" amplitudes produced are identical, which indicates that the size of the coil only changes the attenuation voltage value, and does not have a significant impact on the attenuation process and rate.

In order to obtain the relationship between the coil side length and the attenuation voltage value, the voltage values were chosen at the 10th, 12th, 15th and 17th measurement channels within the abnormal response time to fit the relationship between the two, and the corresponding fitting curve is shown in Figure 8(a)-8(f).

The results show that the attenuation voltage response values corresponding to the six types of mined-out areas all increase in a quadratic function with increasing the side length of the transmitting coil. The attenuation voltage values continue to decrease with the passage of sampling time (the number of time channels increases). The tangent slope of the quadratic formula keeps getting smaller, but the overall growth trend has not changed. In addition, the tangent slopes of the fitting curves of the 4 fitting curves under the 100% water-accumulated condition (including the model with the collapsed body) are the maximum. The tangent slopes of the 4 fitting curves under the condition of the 50% water-accumulation (including the collapsed body model) are the mediate. The slope of the tangent line is the minimum under the condition of no water accumulation (including the model with collapsed body).

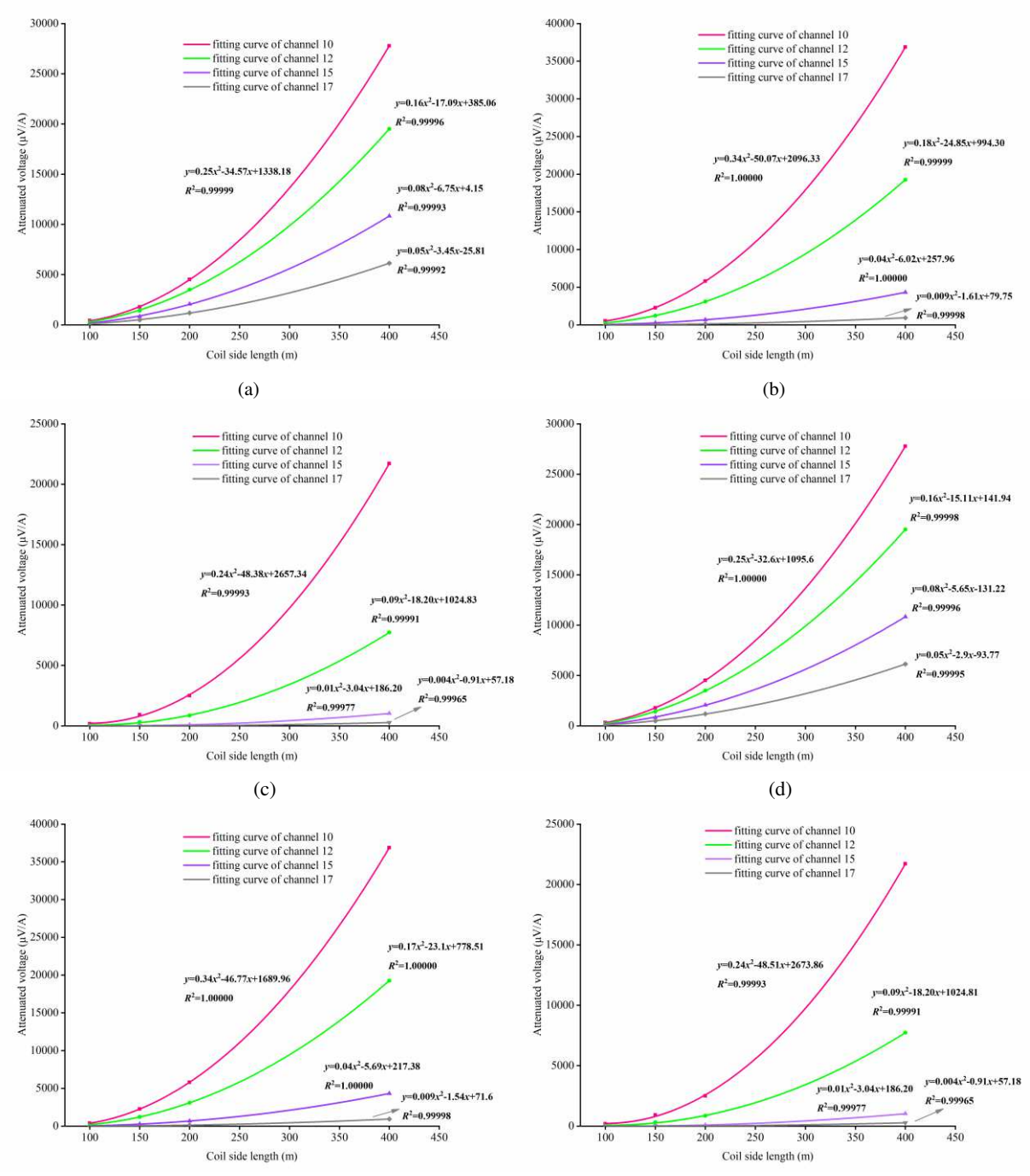


**Fig.8** Fitting curves of the attenuation voltage of the different models: (a) Model of the 100% water accumulation goaf, (b) Model of the 50% water accumulation goaf, (c) Model of the 0% water accumulation goaf, (d) Model of the 100% water accumulation with collapsed rock goaf, (e) Model of the 50% water accumulation with collapsed rock goaf, (f) Model of the 0% water accumulation with collapsed rock goaf

### 3.4 Transient electromagnetic response characteristics of water-filled goaf under different buried depths

This section studies the electromagnetic response characteristics of six goaf models under different transmitter coil sizes. The working parameters are set as follows: the emission current is 1A, the emission frequency is 8Hz, the number of turns is 1, the sampling time is 53ms, and the number of time channels is 30. We choose a 100m×100m square coil for the transmitting coil, and a probe with an equivalent area of 10000m$^2$ for the receiving coil. The buried depth of the water-filled goaf is set to 100m, 150m, 200m and 300m respectively to perform forward calculations on each goaf model, as shown in Figure 9(a)~(f).

It can be seen that the voltage response value during the whole attenuation process decreases with the increase of the buried depth of the goaf, the abnormal amplitude of the "upward convexity" of the curve is reduced accordingly. At the same time, the abnormality of the curve and the increase in response value decrease with the increase of buried depth. This is because the intensity of the transient electromagnetic field signal gradually weakens when it penetrates the rock formations, and the ability to interpret low resistance anomalies will continue to decrease as the depth increases. The shallower the buried depth of the goaf, the shorter the abnormal response duration. When the buried depth reaches 300m, the attenuation voltage response is already extremely weak, and the abnormal phenomenon is not obvious. The above results indicate that the transient electromagnetic exploration has limited detection capabilities for abnormal objects, and the buried depth of the target body will also affect the response value and decay rate of the attenuation voltage.

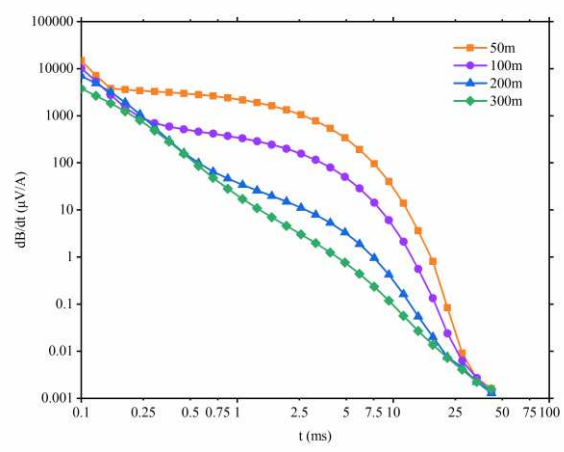


(a)

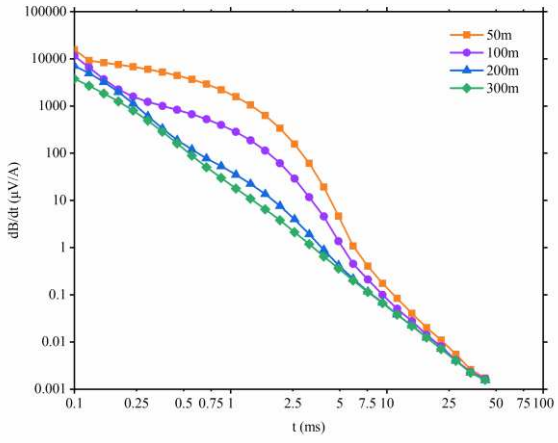


(b)

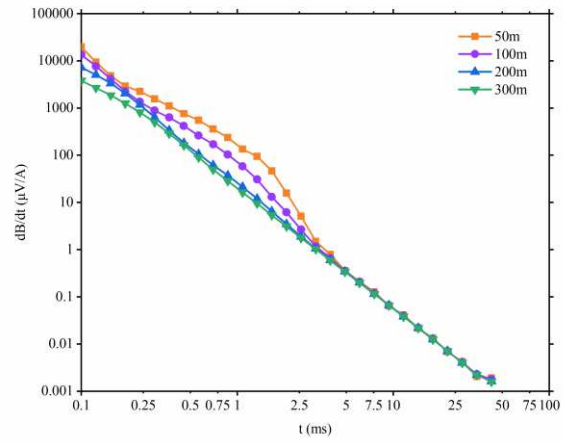


(c)

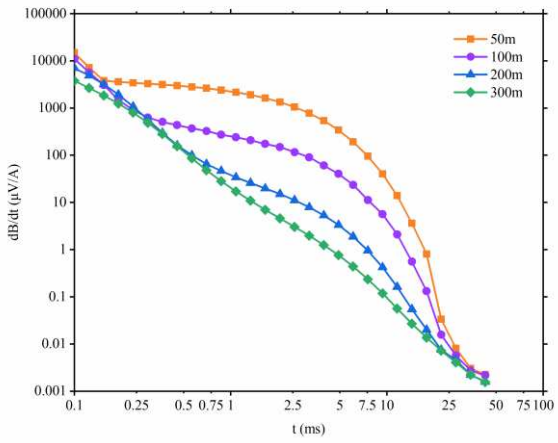


(d)

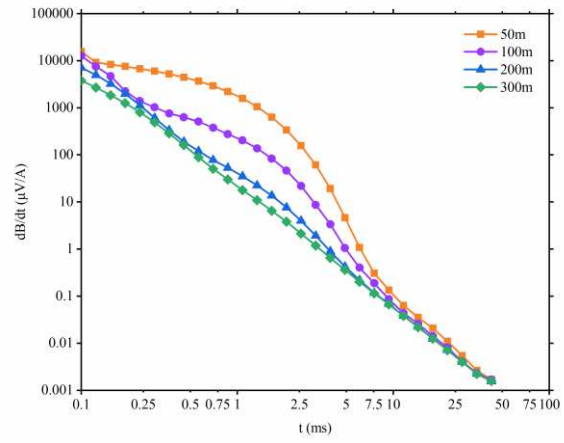


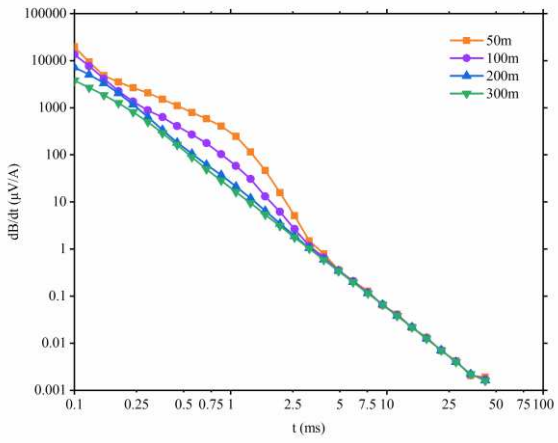

(e) (f)

**Fig.9** Attenuated voltage curves of the different water-filled goaf models with different burial depths: (a) Model of the 100% water accumulation goaf, (b) Model of the 50% water accumulation goaf, (c) Model of the 0% water accumulation goaf, (d) Model of the 100% water accumulation with collapsed rock goaf, (e) Model of the 50% water accumulation with collapsed rock goaf, (f) Model of the 0% water accumulation with collapsed rock goaf

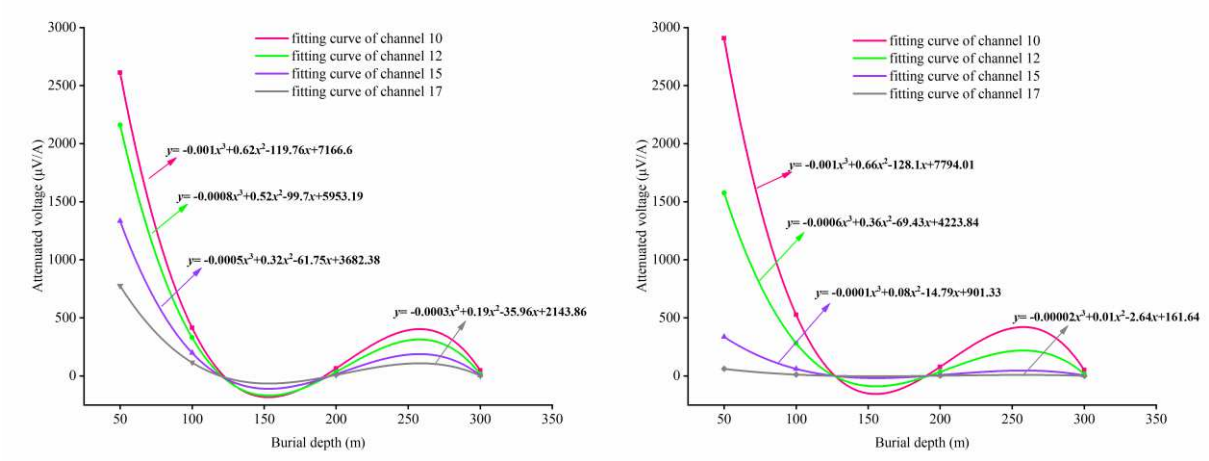


(a)




(b)

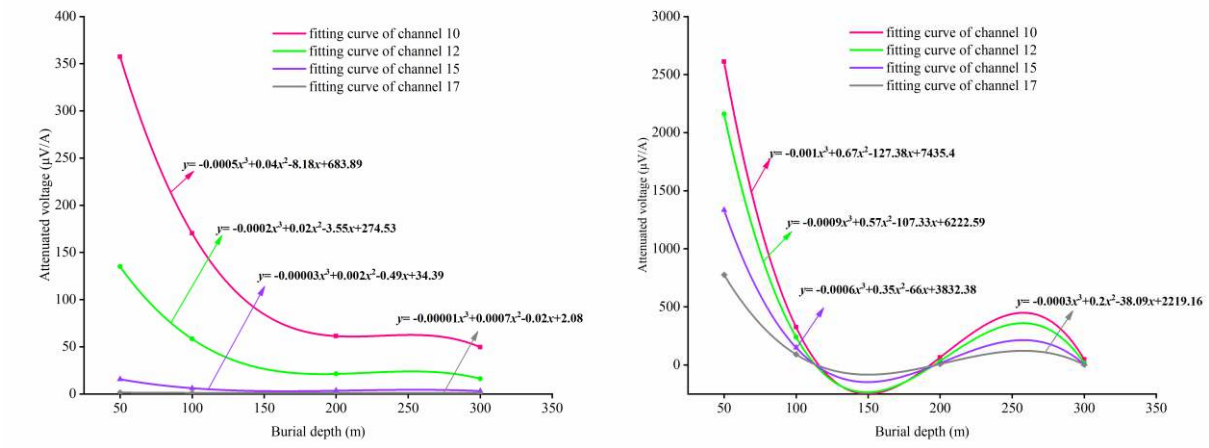


(c)




(d)

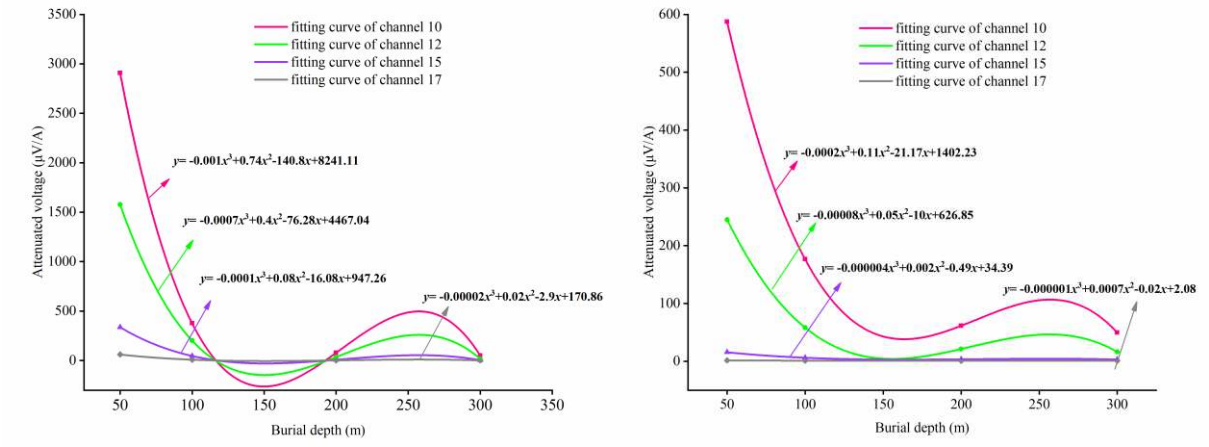


(e)




(f)

**Fig.10** Fitting curves of the attenuation voltage of with different burial depths: (a) Model of the 100% water accumulation goaf, (b) Model of the 50% water accumulation goaf, (c) Model of the 0% water accumulation goaf, (d) Model of the 100% water accumulation with collapsed rock goaf, (e) Model of the 50% water accumulation with collapsed rock goaf, (f) Model of the 0% water accumulation with collapsed rock goaf

In order to obtain the relationship between the buried depth and the attenuation voltage value, the 10th, 12th, 15th and 17th measurement channels of voltage values were seleted within the abnormal response time to fit the relationship between the two, and the corresponding fitting curve is shown in Figure 10(a)-10(f).

The results show that the attenuation voltage response values corresponding to the 6 types of mined-out areas decrease in a cubic function with the increase of the buried depth of the detection target. The fitting curves of the 4 measuring tracks under the fully accumulated water condition (including the model with the collapsed body) have the largest decrement in the buried depth from 50m to 150m. The change range of the four fitting curves under the 50% water accumulation (including the model with the collapsed rock) is second, and the variation range under the condition of no water accumulation (including the model with the collapsed body) is the minimum.

## 4 Field application

### 4.1 Geological conditions of the mining area

The Majiliang Minefield is located in the west of the Jurassic boundary of the Datong Coalfield, and belongs to the central and western wing of the Datong syncline. The exploration area is the Carboniferous $8^{\#}$ coal seam, which is located in the lower part of the Taiyuan Formation, generally about 15m from the bottom of the K2 sandstone, and 18m from the $5^{\#}$ coal seam. The thickness of the coal seam is 1.25-18.77m, with an average of 8.38m. The $8^{\#}$ coal seam is stable and simple in structure. and contains 0 to 2 layers of gangue. In the eastern part of the minefield, it suffers from lamprophyre intrusion and damage to the coal seam, which has a large impact area. Also, it is one of the main mineable and stable coal seams in this area. Due to the uncertainty of the small coal kiln excavation in the early stage, the location of the mining area and the water accumulation situation are uncertain. Therefore, the scope of the goaf of water accumulation should be explored.

### 4.2 Probe preparation and instrument selection

In this field experiment, the V8 multifunctional transient electromagnetic system was selected for ground transient electromagnetic detection. According to the actual geological conditions of the Majiliang mining area and multiple parameter optimization tests, we determined the final working parameters. The transmitter adopts T-4A transient electromagnetic emission, the coil is a square coil with a side length of 300m, and the receiving device is replaced by a receiving coil with an equivalent area of $100m^2$. The operating frequency is 25Hz, the transmitting current is 9A, and the gain is 1. The prospecting area distributed on the 8111 working surface on the southeast side of the mining area, and the survey area is about $1.21km^2$.

The experiment uses a 20m×20m network type (which the line spacing is 20m, and the point spacing is 20m) to lay out the survey lines and points. A total of 3536 measurement points are arranged on the 8111 working surface to ensure uniform coverage of the entire measurement area. Meanwhile, according to the information provided by the mine, the location of the predicted water-filled goaf was analyzed and generated the site layout of the 8111 working face as shown in Figure 11. The green box represents the detection coil, the internal numbers indicate the detection sequence, the pink dotted line represents the entire transient electromagnetic exploration boundary, the red cross represents the location of the measurement point, the black dotted line represents the coal seam boundary, and the number on the frame of the map represents the coordinate value of the mining area.

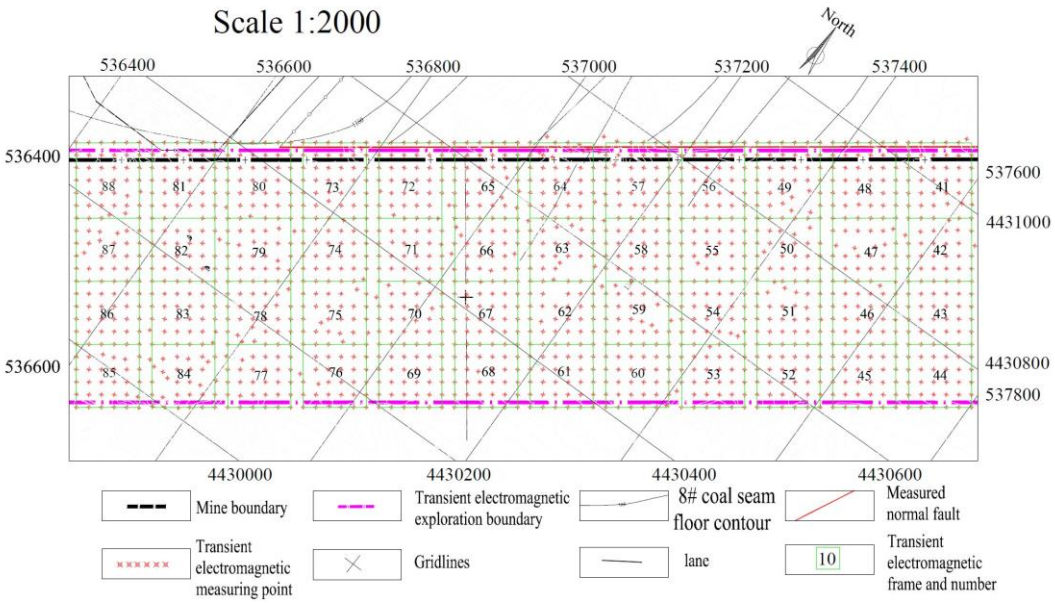


**Fig.11** Layout drawing of site detection on 8111 working face

### 4.3 results and analysis

After forward calculation and noise reduction processing, the attenuation voltage curves of the three regions are obtained, and corresponding to the region called L8-1, L8-2, and L8-3 as shown in Figure 12. Among them, curves L8-2 and L8-3 have a "bump" phenomenon at the sampling time of 0.27ms to 2.28ms. The voltage response value rises sharply during this period, indicating that the two curves are affected by the low resistance abnormal effect and hinder the normal attenuation process. At the same time, the sequence of the abnormal amplitude about the three curves is L8-3>L8-2>L8-1, while the voltage response value during the abnormal time also follows the above relationship.

In line with the attenuation voltage curve under different water accumulation conditions of goaf obtained by numerical simulation and theoretical calculation, it can be inferred that the area where L8-2 and L8-3 located is water-filled goaf, and the area where L8-1 located is water-unfilled goaf. And the water accumulation degree in the area where the curve L8-3 is located is greater than that of the curve L8-2.

Based on the above forward simulation results, the apparent resistivity cross-section of No. 8 coal seam in the 8111 working face is drawn in Figure 13. The numbers outside the block diagram are the position coordinates of the detection area. The blue to red in the figure indicates that the apparent resistivity decreases from low to high, and blue low-resistance area represents the range of water-filled goaf (excluding high-voltage line interference area). Meanwhile, 70Ω·m is used as the threshold for the low-value abnormality of apparent resistivity. The figure divides three low-resistance areas. where numbered L8-1, L8-2, and L8-3. It can be seen from the figure that the area and amount of accumulated water in the L8-3 area are the largest, the second is L8-2. The area of L8-1 is smaller and the amount of water contained in the former is negligible. It is inferred that there is no accumulated water in the mined area of L8-3. At last, the accuracy of the detection results was also verified after drilling.

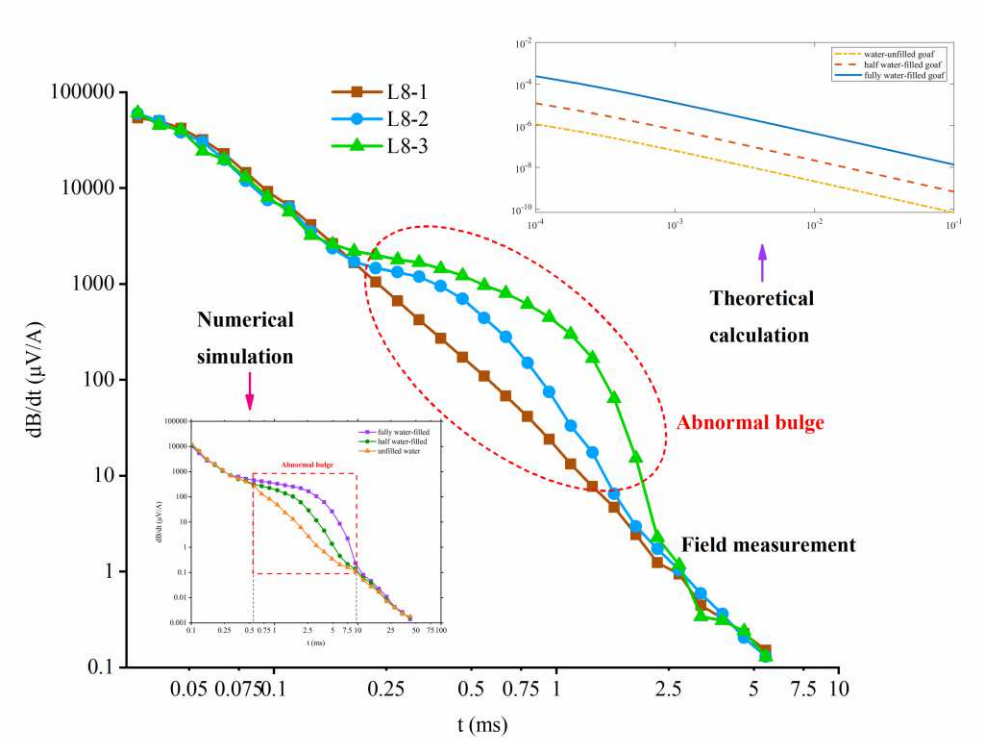


**Fig.12** Attenuation voltage curves under different measurement locations on 8111 working face and comparison analysis chart with numerical simulation and theoretical calculation

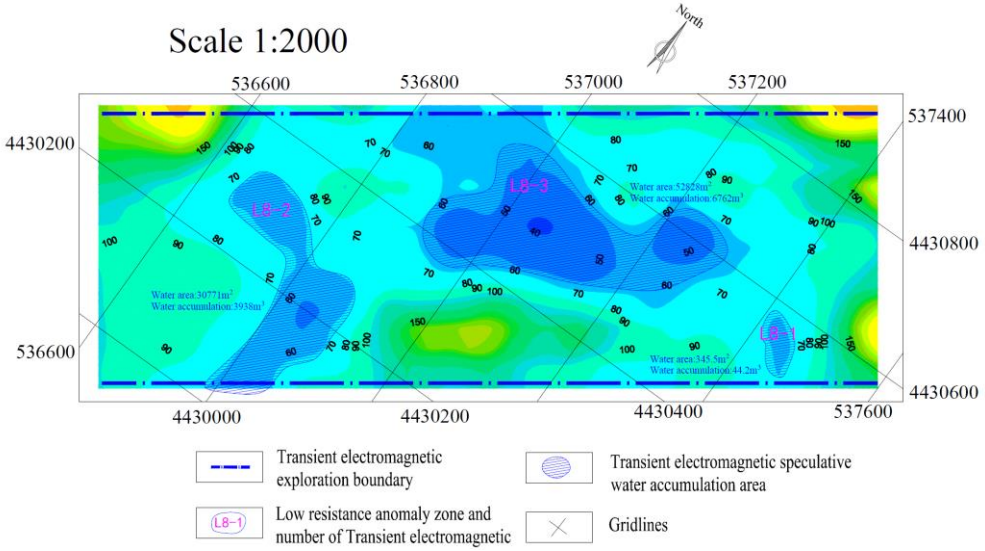


**Fig.13** Apparent resistivity profile of 8# Coal Seam on 8111 Working Face

## 5 Conclusion

(1) Based on Maxwell's equations, the transient electromagnetic detection theory of the goaf with water accumulation is derived, and the expression of the induced electromotive force is obtained. At the same time, Matlab software is used to calculate the change characteristics of the attenuation voltage response curve of the goaf with different water accumulation.

$$\frac{\partial B_z(t)}{\partial t}=\mu\frac{\partial H_z(t)}{\partial t}=\frac{3I_0\rho_w(3-\omega)}{2\omega a^3}\left[\Phi(u)-\sqrt{\frac{2}{\pi}}u\left(1+\frac{u^2}{3}\right)e^{-\frac{u^2}{2}}\right]$$

(2) According to the geology background of the Majiliang Coal Mine, goaf model with six water accumulation situation were built as 100% water accumulation, 50% water accumulation, 0% water accumulation, 100% water accumulation with collapsed rock,

50% water accumulation with collapsed rock and 0% water accumulation with collapsed rock goaf models. The simulation results demonstrate that the TEM detection has strong resolution in the low-resistance water-filled goaf and would generate obvious abnormal reactions. The attenuation curve presents a third-order exponential function distribution, and the distribution form is "S". However, the resolution of the goaf without water content is poor, and there is no abnormality in the curve during the decay process, which follows the normal exponential decay pattern. At the same time, the larger the water accumulation could lead to higher the abnormal amplitude and greater the voltage response value. The collapsed rock wound slightly weaken the low-resistance anomaly effect in the water-accumulated mine-out area.

(3) The transient electromagnetic response characteristics of each goaf model under different working parameters are studied. The response value of the attenuation electromotive force increased as a quadratic polynomial with the rise of the area of the detection coil, and the response value of the attenuation electromotive force decreases as a third polynomial with the increasing of the buried depth.

(4) The results of the attenuation curve of theoretical analysis and numerical simulation were verified through field detection experiment of Majiliang coal mine. Meanwhile, the research results of this paper provide theoretical and technical guidance for the accurate detection and effective treatment of water-filled goaf.

**Acknowledgements**

The project was supported by the Joint Funds of National Natural Science Foundation of China and Shanxi Province (U1710258), Distinguished Youth Funds of National Natural Science Foundation of China (51925402), Key Research and Development Project of Shanxi (201803D31044) and National Natural Science Foundation of China (51804208).

**Declarations**

The authors declare that they have no conflict of interest.

**References**

Wang P, Chen J Y, Yao W H (2019) Technology of detecting water-filled goaf beside borehole using downhole transient electromagnetic method. Journal of China Coal Society 44(8): 2502-2508.

Dong S N (2007) Coal mine water hazard prevention tech nology and application, Safety and efficient coal mine geological support technology and application// China Coal Industry Labor Protection Science and Technology Society Water Hazard Prevention Committee Proceedings of the Academic Annual Conference, Beijing: China Geological Society, China Coal Society Coalfield Geology Committee.

Shan L, Xu R K, Lu S Z, et al. (2009) The Transient Elec tromagnetic Method: Principle, current situation and application in mineral exploration. Geology and Resources 18(1): 70-73.

Liu S D, Liu J, Yue J H (2014) Development status and key problems of Chinese mining geophysical technology. Journal of China Coal Society 39(1): 19-25.

Fitterman D V, Menges C M, Aikamali A M, et al. (1991) Electromagnetic Mapping of Buried Paleochannels in Eastern Abu Dhabi Emirate U A E. Geoexploration 27(1-2): 111-133.

Taylor K, Widmer M, Chesley M (1992) Use of transient electromagnetic to define local hydrogeology in an arid alluvial environment. Geophysics 57: 343–352.

Garg N R, Keller G V (1999) Spatial and temporal analysis of electromagnetic survey data. Geophysics 51(1): 85-89.

Abu Rajab J S, El-Naqa A R (2013) Mapping groundwater salinization using transient electromagnetic and direct current resistivity methods in Azraq Basin, Jordan. Geophysics 78: B89–B101.

Chang J H, Su B Y, Malekian R, et al (2019) Detection of water-filled mining goaf using mining transient electromagnetic method. IEEE Transactions on Industrial Informatics (99): 1-1.

Li C Y, Liu H F (2007) The Application of Transient Elec tromagnetic Method to The Detection of Multilayer Worked-out Aera of Coal Seam. Geophycial & Geochemical Exploration 31(S1): 108-110.

Jiang Z H, Yang G (2014) Research and application of TEM detection technology for small mine gob area in shallowly-buried and extremely thick seam. Journal of Mining & Safety Engineering 31(5): 769-774.

Tang Z Y, Zhang H, Gong Y L (2015) The Application of Transient Electromagnetic Imaging Technology to Goaf

Water. Chinese Journal of Engineering Geophysics 12(5): 633-636.

Chang J H, Yu J C, Su B Y (2017) Numerical Simulation and Application of Mine TEM Detection in a Hidden Water-bearing Coal Mine Collapse Column. Environmental and Engineering Geophysics 22(3): 223-234.

Yu C T, Liu X Y, Liu J S, et al. (2018) Application of Transient Electromagnetic Method for Investigating the Water-Enriched Mined-Out Area. Applied Sciences 8(10): 1800-1811.

Yan G C, Xian P H, Qiu N G (2020) Study on short offset transient electromagnetic detection technology for low －resistance electrical sources in deep mine. Coal Science and Technology 48 (6): 171-176.

Li Yuan (2002) The Theory and Application of Transient Electromagnetic Sounding. Shaanxi Science and Technology Press, Xi'an.

Luo H G (2012) The Study about 1D Forward Modeling of Large-fixed Loop TEM. China University of Geosciences, Beijing.

Bai D H, Maxwell M A, Lu J, et al. (2003) Numerical Calcu lation of All-time Apparent Resistivity For The Central Loop Transient Electromagnetic Metho. Chinese Journal of Geophysics 46(5): 697-704.

Tong X Z, Liu J X (2013) MATLAB programming and its application in geophysics.: Central South University Press, Changsha.

Han Y (2018) The Research on Abnormal Range of Central Loop by Transient Electromagnetic Method. Taiyuan University of Technology, Taiyuan.

Lian X, Hu H , Li T , et al. (2020) Main geological and mining factors affecting ground cracks induced by underground coal mining in Shanxi Province, China. International Journal of Coal Science & Technology (prepublish).

# Figures

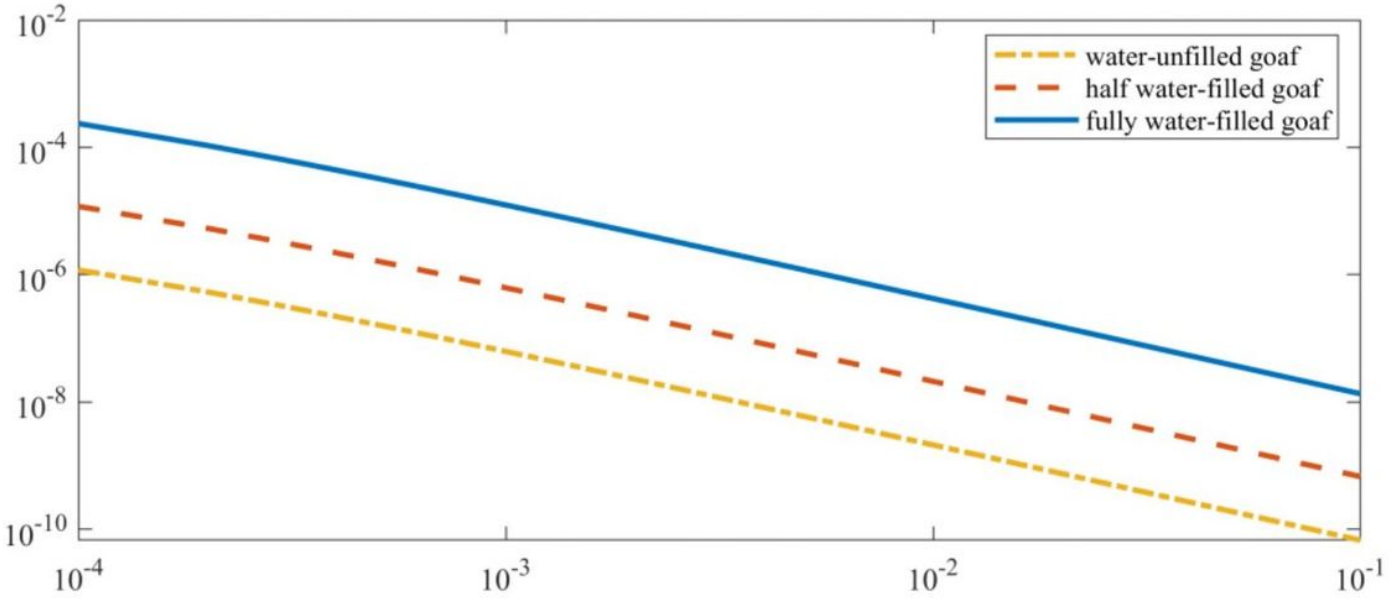


**Figure 1**

Attenuated voltage curve of the water-filled goaf under different states

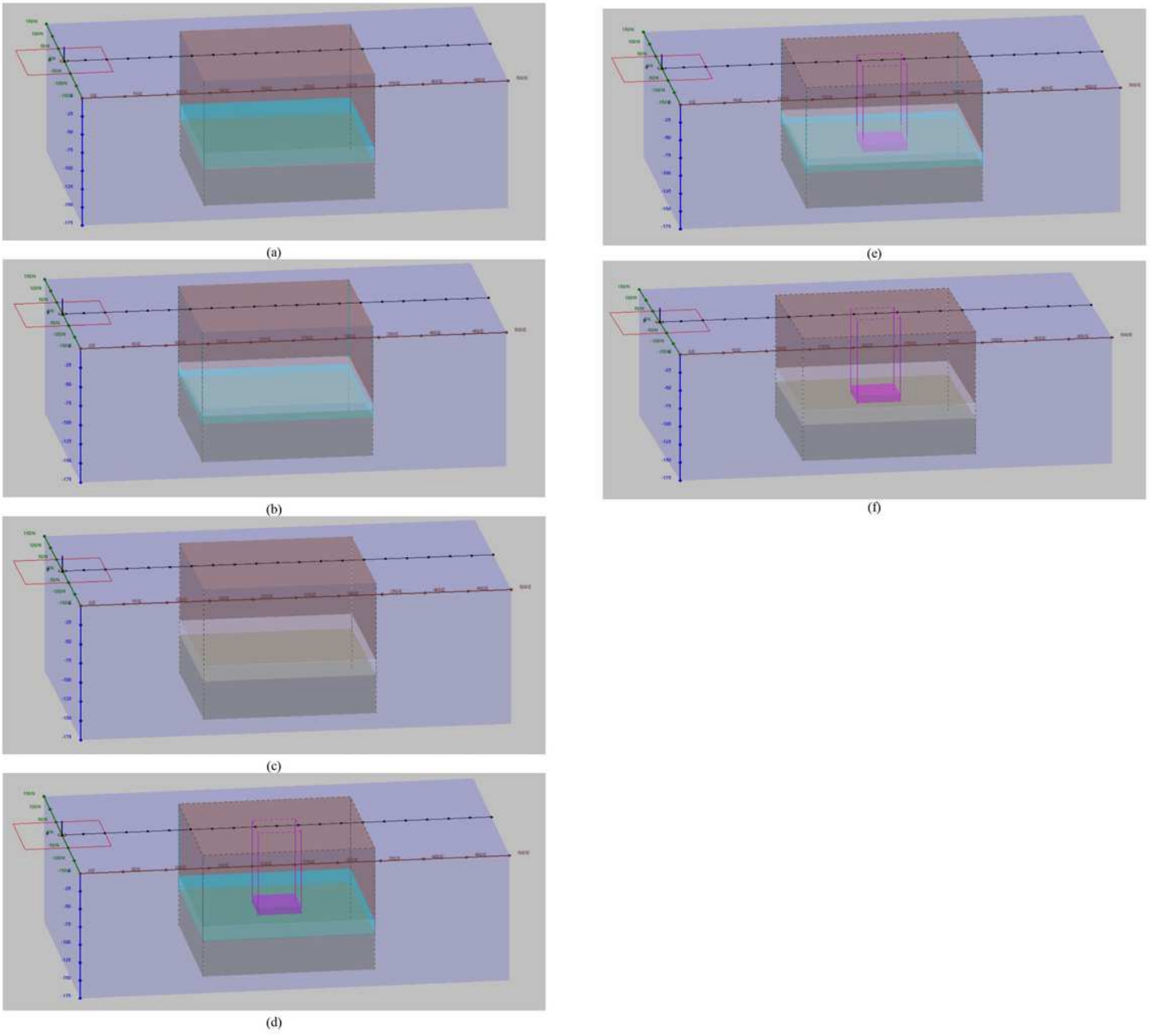


## Figure 2

Model of the water-filled goaf under different states: (a) Model of the 100% water accumulation goaf, (b) Model of the 50% water ac-cumulation goaf, (c) Model of the 0% water accumulation goaf, (d) Model of the 100% water accumulation with collapsed rock goaf, (e) Model of the 50% water accumulation with collapsed rock goaf, (f) Model of the 0% water accumulation with collapsed rock goaf

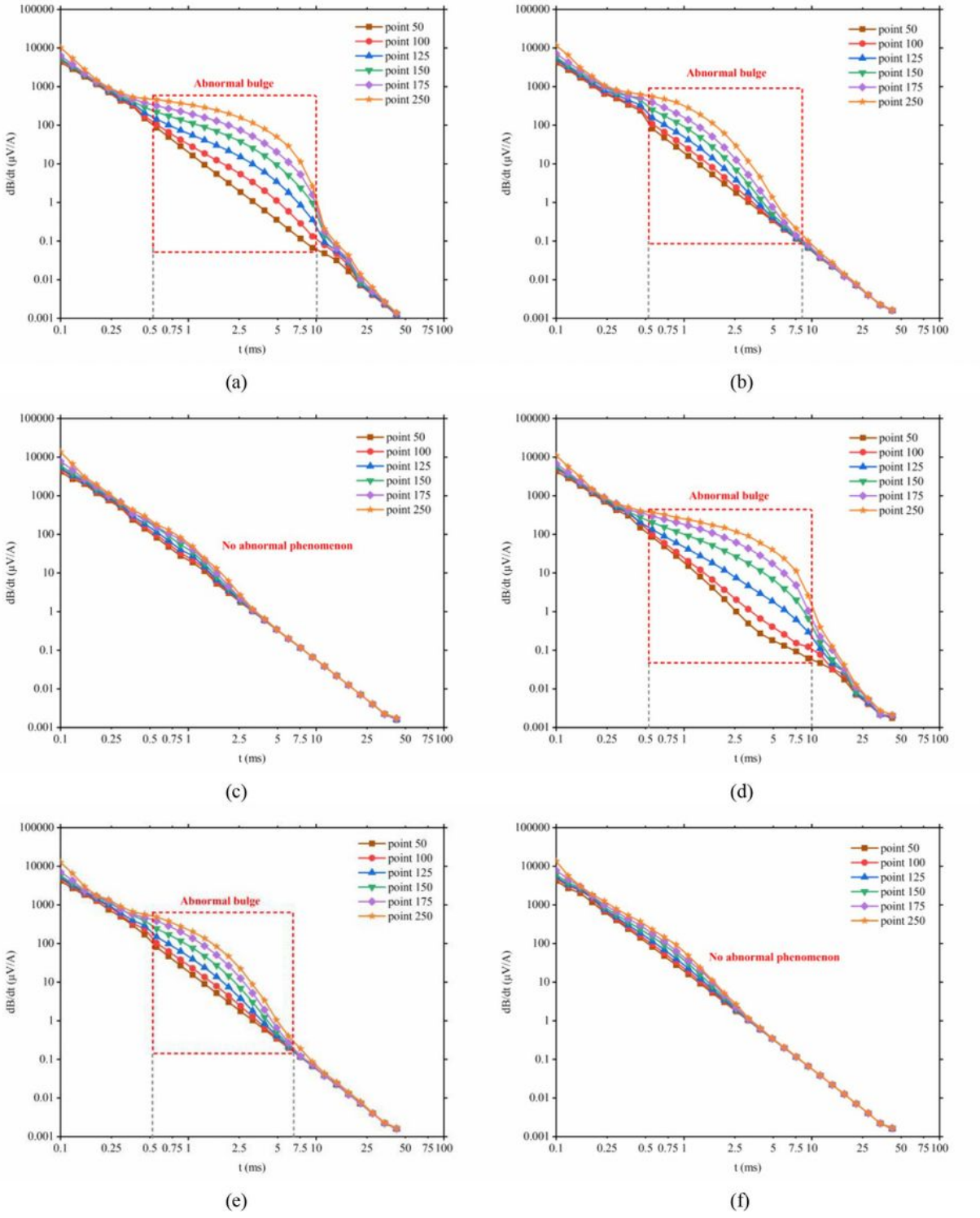


## Figure 3

Attenuated voltage curve of water-filled goaves in different states: (a) Model of the 100% water accumulation goaf, (b) Model of the 50% water accumulation goaf, (c) Model of the 0% water accumulation goaf, (d) Model of the 100% water accumulation with collapsed rock goaf, (e) Model of the 50% water accumulation with collapsed rock goaf, (f) Model of the 0% water accumulation with collapsed rock goaf

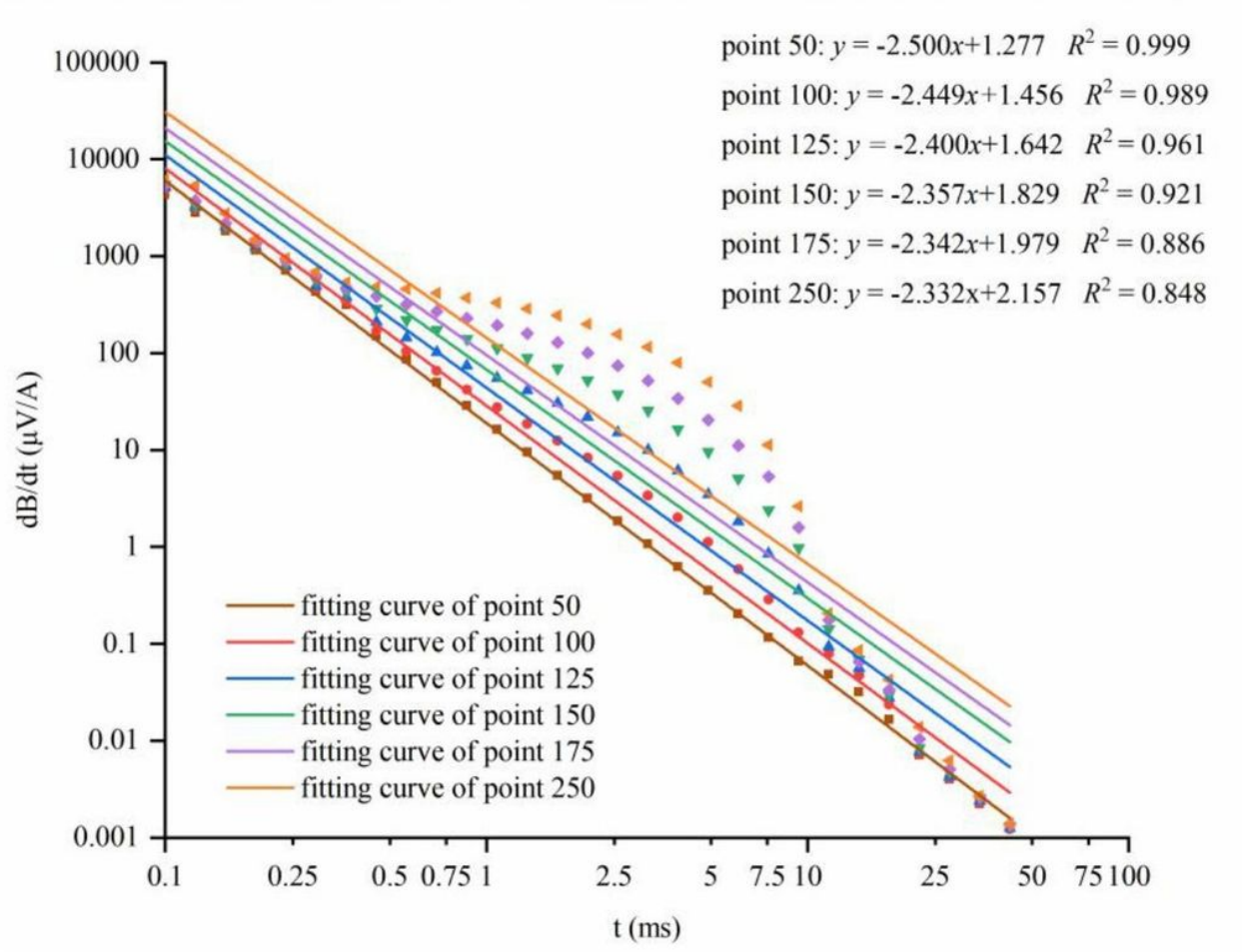


**Figure 4**

The fitting curve of the attenuation voltage of measuring points in 100% water accumulation goaf

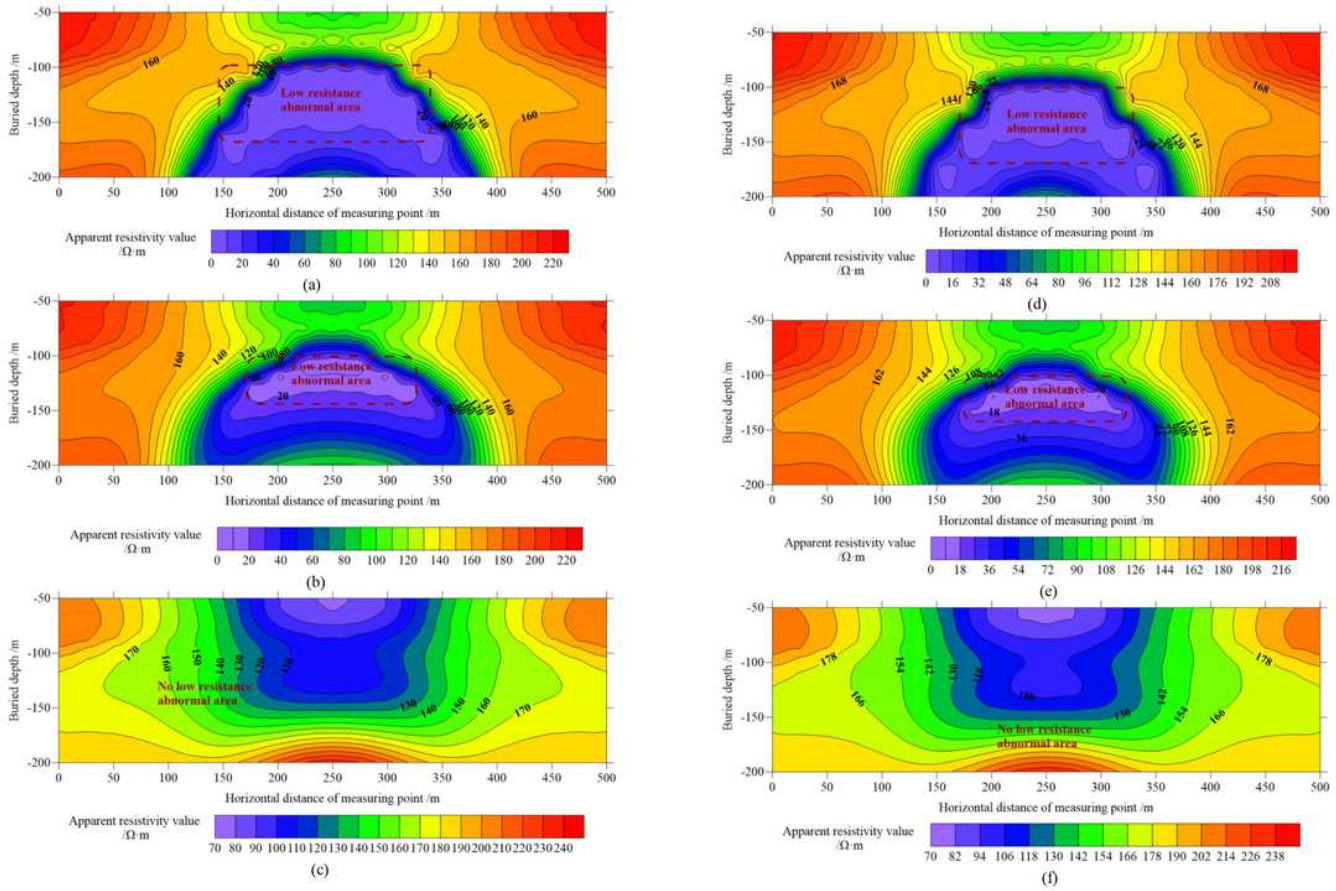


## Figure 5

The apparent resistivity cross-section diagrams of the goaf with water accumulation in different states: (a) Model of the 100% water accumulation goaf, (b) Model of the 50% water accumulation goaf, (c) Model of the 0% water accumulation goaf, (d) Model of the 100% water accumulation with collapsed rock goaf, (e) Model of the 50% water accumulation with collapsed rock goaf, (f) Model of the 0% water accumulation with collapsed rock goaf

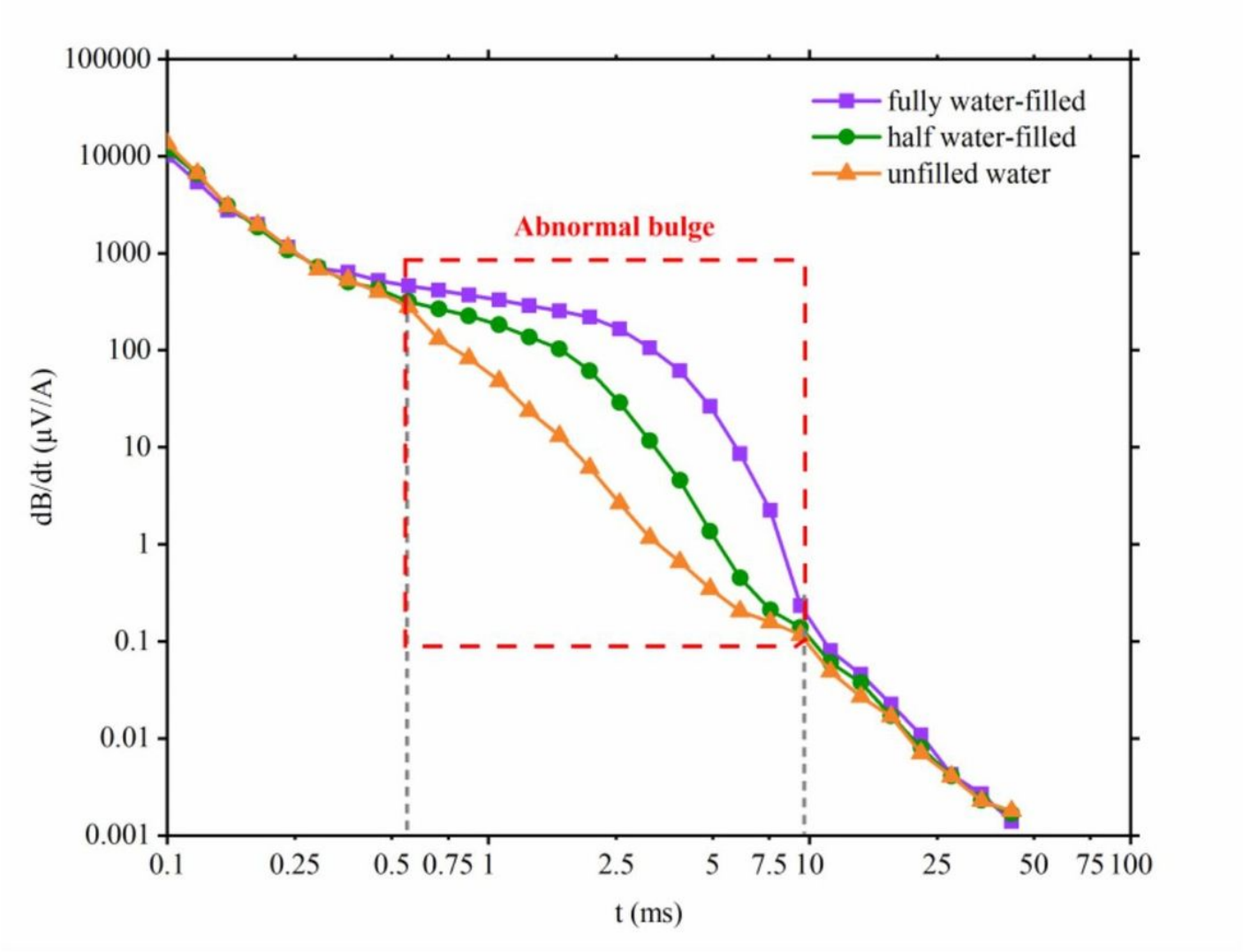


**Figure 6**

Attenuation voltage curves under different amounts of accumulated water

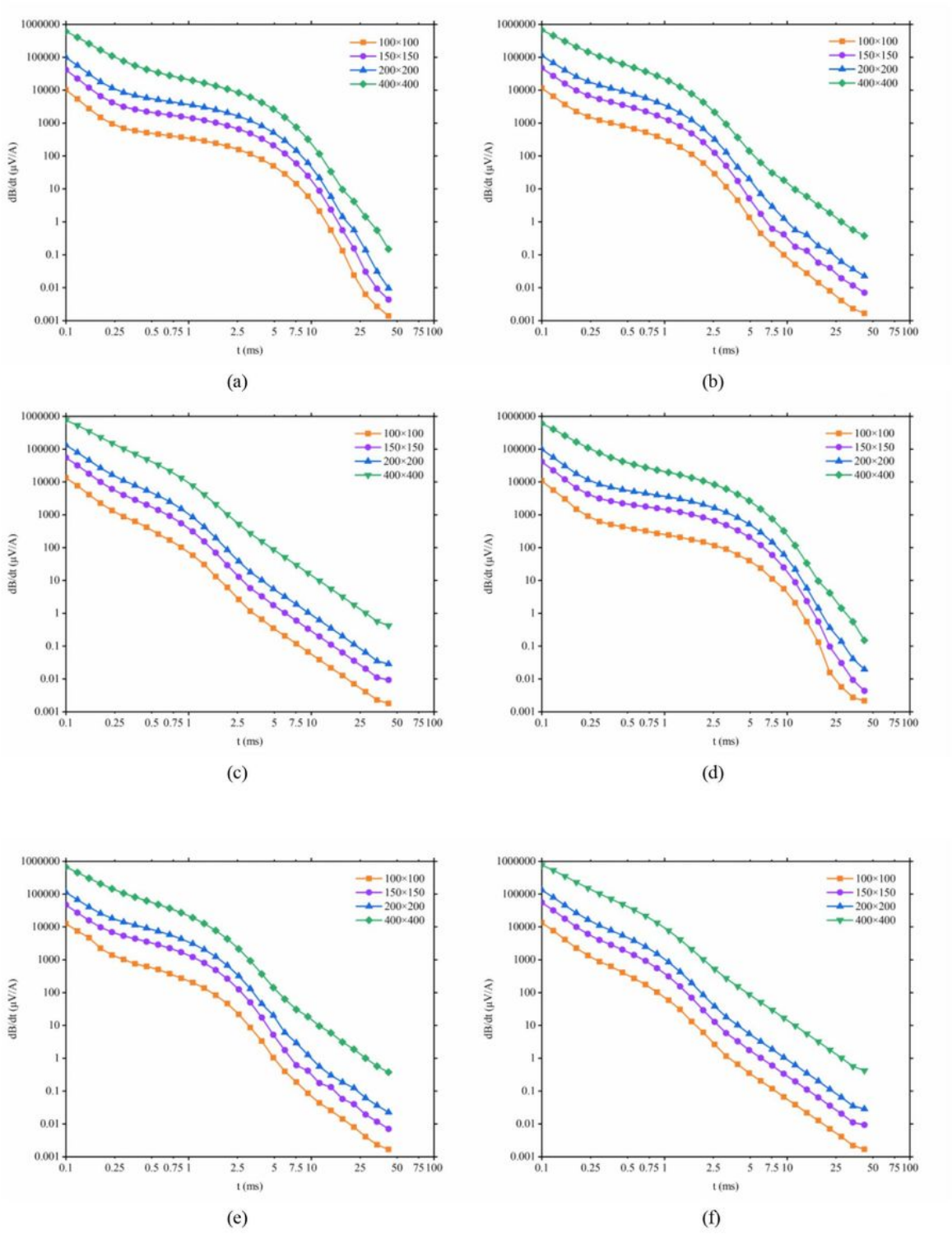


## Figure 7

Attenuated voltage curves of the different water-filled goaf models with different coil sizes: (a) Model of the 100% water accumulation goaf, (b) Model of the 50% water accumulation goaf, (c) Model of the 0% water accumulation goaf, (d) Model of the 100% water ac-cumulation with collapsed rock goaf, (e) Model of the 50% water accumulation with collapsed rock goaf, (f) Model of the 0% water accumulation with collapsed rock goaf

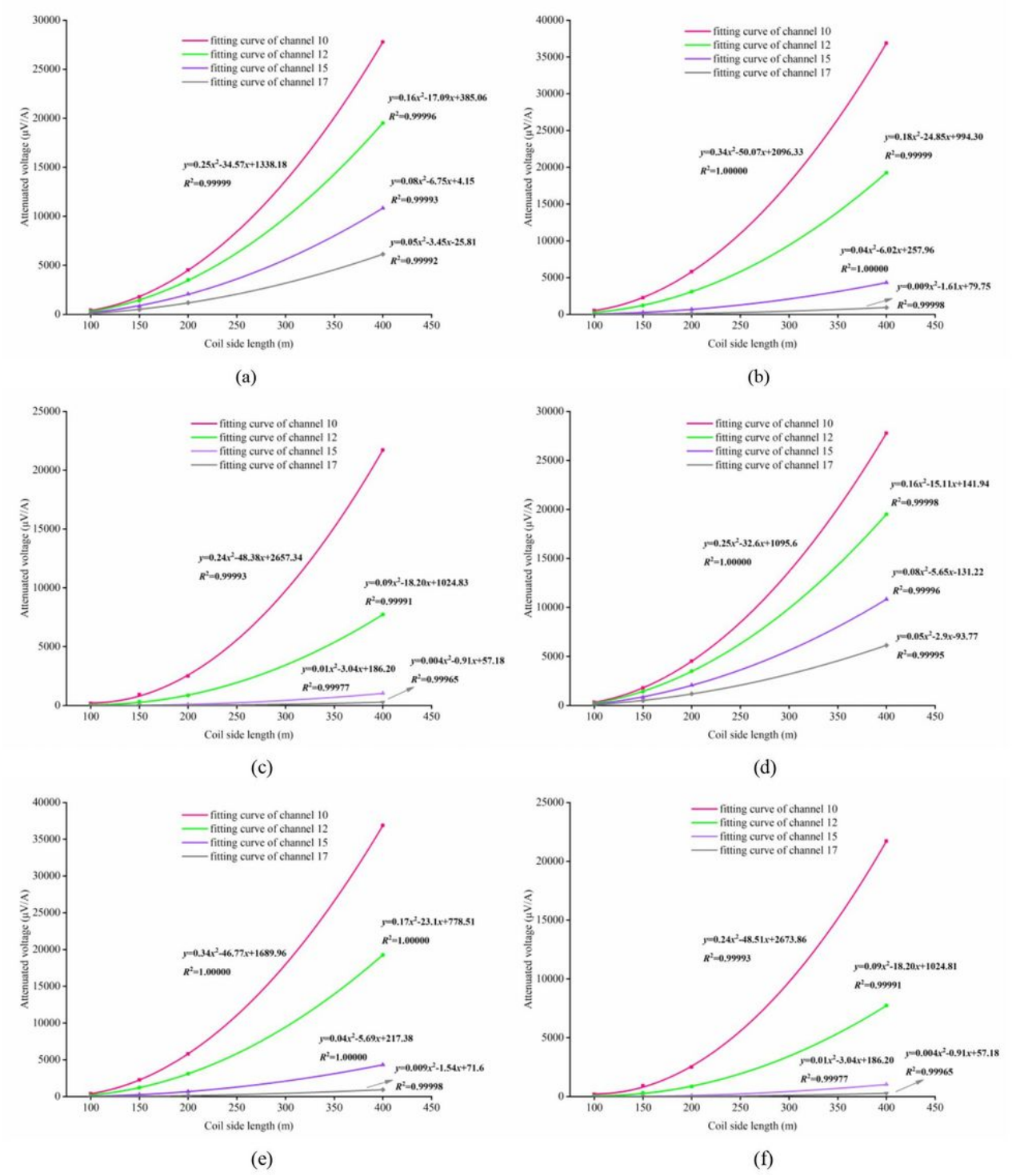


## Figure 8

Fitting curves of the attenuation voltage of the different models: (a) Model of the 100% water accumulation goaf, (b) Model of the 50% water accumulation goaf, (c) Model of the 0% water accumulation goaf, (d) Model of the 100% water accumulation with collapsed rock goaf, (e) Model of the 50% water accumulation with collapsed rock goaf, (f) Model of the 0% water accumulation with collapsed rock goaf

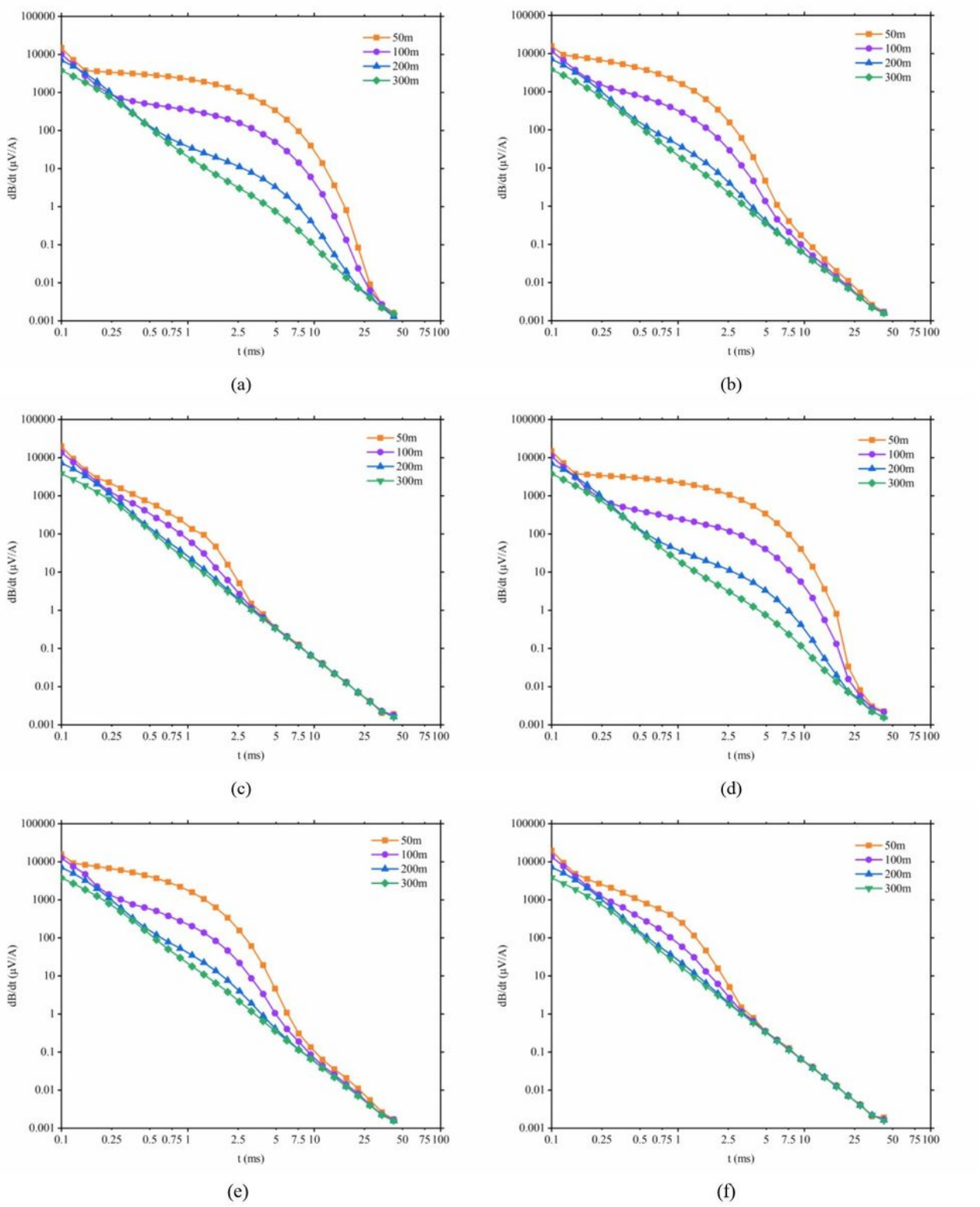


**Figure 9**

Attenuated voltage curves of the different water-filled goaf models with different burial depths: (a) Model of the 100% water accumula-tion goaf, (b) Model of the 50% water accumulation goaf, (c) Model of the 0% water accumulation goaf, (d) Model of the 100% water accumulation with collapsed rock goaf, (e) Model of the 50% water accumulation with collapsed rock goaf, (f) Model of the 0% water accumulation with collapsed rock goaf

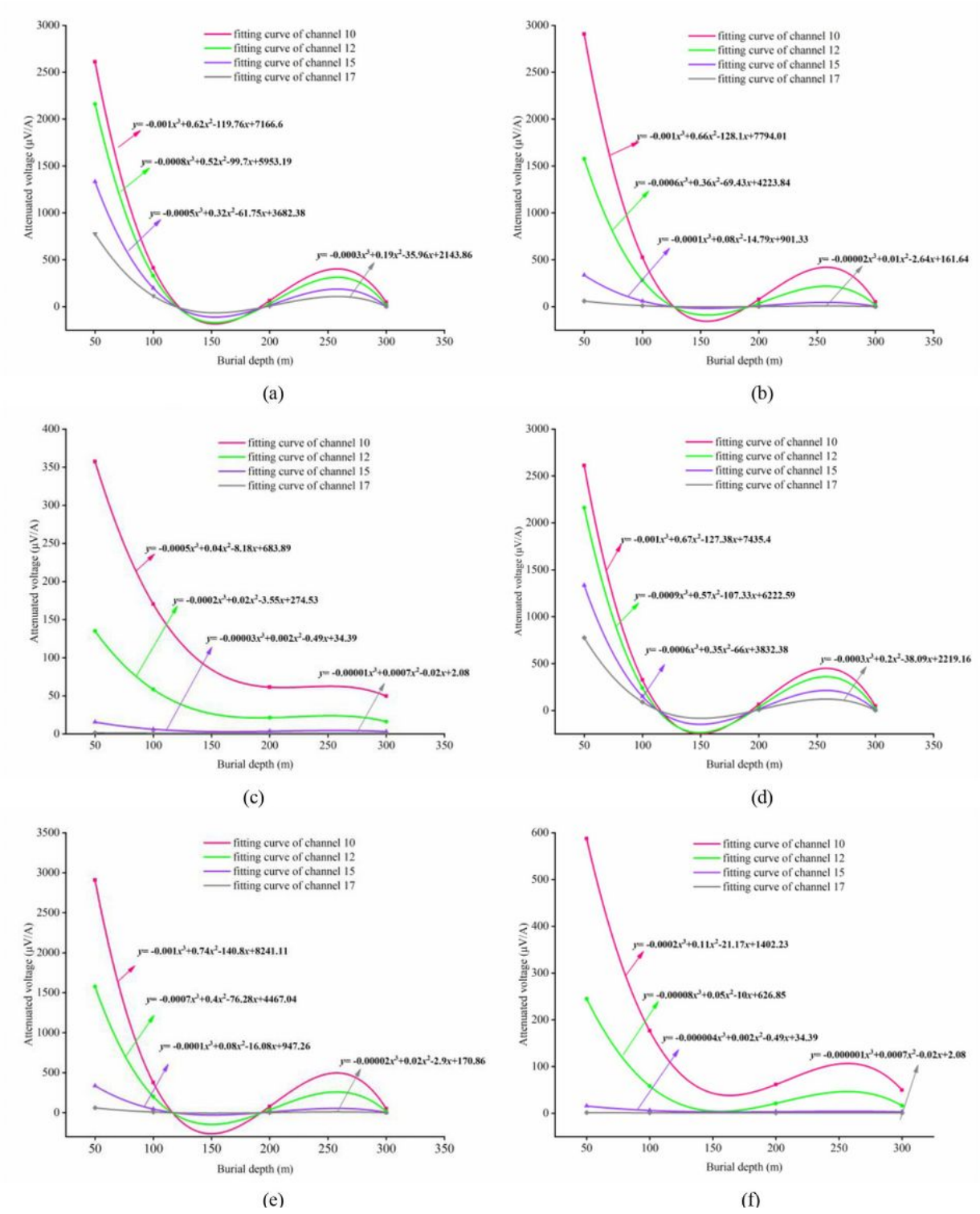


**Figure 10**

Fitting curves of the attenuation voltage of with different burial depths: (a) Model of the 100% water accumulation goaf, (b) Model of the 50% water accumulation goaf, (c) Model of the 0% water accumulation goaf, (d) Model of the 100% water accumulation with col-lapsed rock goaf, (e) Model of the 50% water accumulation with collapsed rock goaf, (f) Model of the 0% water accumulation with collapsed rock goaf

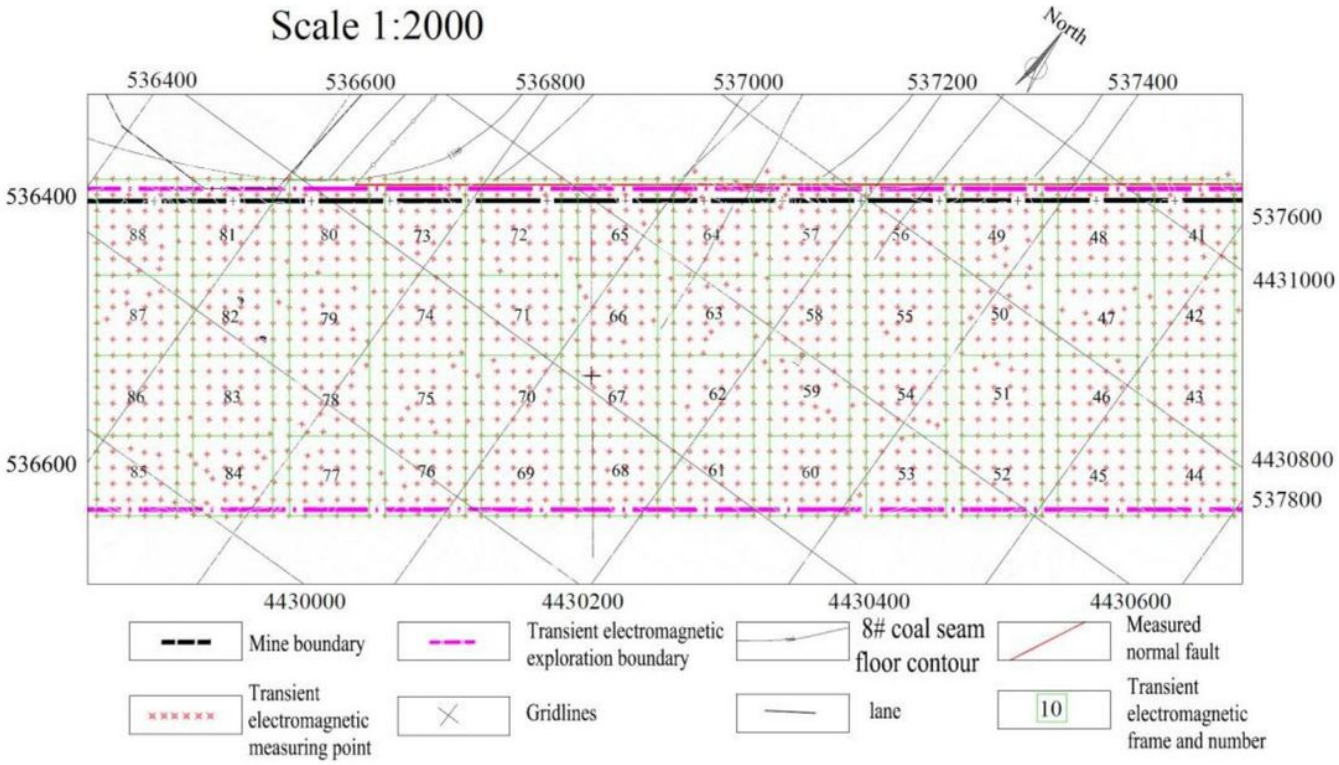


**Figure 11**

Layout drawing of site detection on 8111 working face

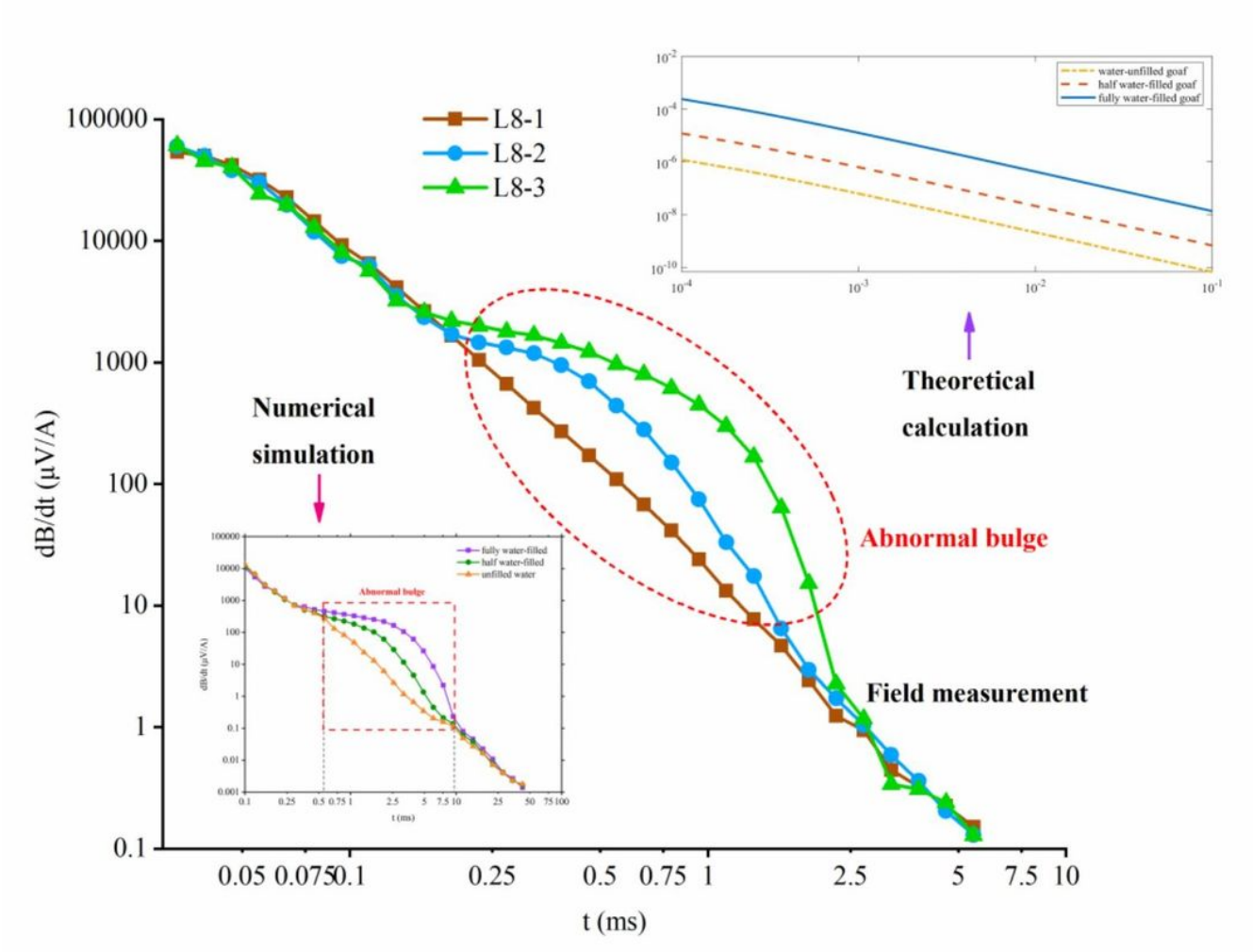


**Figure 12**

Attenuation voltage curves under different measurement locations on 8111 working face and comparison analysis chart with numerical simulation and theoretical calculation

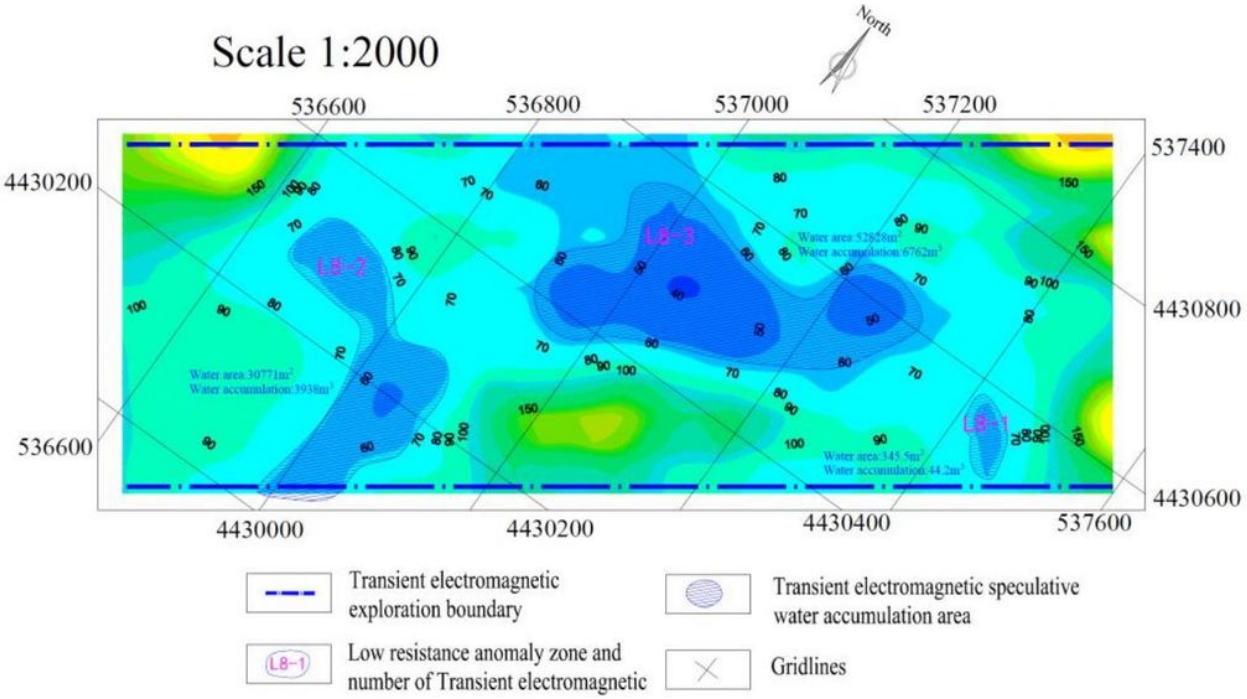


**Figure 13**

Apparent resistivity profile of 8# Coal Seam on 8111 Working Face